THE JOURNAL OF BIOLOGICAL CHEMISTRY VOL. 291, NO. 5, pp. 2444–2459, January 29, 2016

Differential α4(+)/(−)β2 Agonist-binding Site Contributions to α4β2 Nicotinic Acetylcholine Receptor Function within and between Isoforms*

Received for publication, August 7, 2015, and in revised form, November 23, 2015 Published, JBC Papers in Press, December 7, 2015, DOI 10.1074/jbc.M115.684373

Linda M. Lucero[‡], Maegan M. Weltzin[‡], J. Brek Eaton[‡], John F. Cooper[§], Jon M. Lindstrom[§], Ronald J. Lukas[‡], and Paul Whiteaker[‡1]

From the [‡]Division of Neurobiology, Barrow Neurological Institute, Phoenix, Arizona 85013 and the [§]Department of Neuroscience, University of Pennsylvania Medical School, Philadelphia, Pennsylvania 19104

Two α4β2 nicotinic acetylcholine receptor (α4β2-nAChR) isoforms exist with $(\alpha4)_2(\beta2)_3$ and $(\alpha4)_3(\beta2)_2$ subunit stoichiometries and high *versus* low agonist sensitivities (HS and LS), respectively. Both isoforms contain a pair of α4(+)/(−)β2 agonist-binding sites. The LS isoform also contains a unique α4(+)/(−)α4 site with lower agonist affinity than the α4(+)/(−)β2 sites. However, the relative roles of the conserved α4(+)/(−)β2 agonist-binding sites in and between the isoforms have not been studied. We used a fully linked subunit concatemeric nAChR approach to express pure populations of HS or LS isoform α4β2*-nAChR. This approach also allowed us to mutate individual subunit interfaces, or combinations thereof, on each isoform background. We used this approach to systematically mutate a triplet of β2 subunit (−)-face E-loop residues to their non-conserved α4 subunit counterparts or vice versa (β2HQT and α4VFL, respectively). Mutant-nAChR constructs (and unmodified controls) were expressed in *Xenopus* oocytes. Acetylcholine concentration-response curves and maximum function were measured using two-electrode voltage clamp electrophysiology. Surface expression was measured with ^{125}I-mAb 295 binding and was used to define function/nAChR. If the α4(+)/(−)β2 sites contribute equally to function, making identical β2HQT substitutions at either site should produce similar functional outcomes. Instead, highly differential outcomes within the HS isoform, and between the two isoforms, were observed. In contrast, α4VFL mutation effects were very similar in all positions of both isoforms. Our results indicate that the identity of subunits neighboring the otherwise equivalent α4(+)/(−)β2 agonist sites modifies their contributions to nAChR activation and that E-loop residues are an important contributor to this neighbor effect.

Nicotinic acetylcholine receptors (nAChR)[2] are ligand-gated ion channel neurotransmitter receptors. In mammals, they are expressed as pentameric combinations of homologous subunits, translated from 16 different genes (α1–α7, α9, α10, β1–β4, γ, δ, and ϵ). Functional diversity of nAChR is determined by subunit composition, producing nAChR subtypes with overlapping pharmacological and biophysical characteristics (1).

α4β2*-nAChR are the most prevalent central nervous system (CNS) nAChR subtype, comprising ≈70% of all rodent CNS nAChR (2) and are implicated in a wide range of normal and pathological functions, including learning, memory, mood, and nicotine dependence among others (3–17). α4β2*-nAChR functionally interact with nicotine at concentrations found in smokers and are the target of varenicline, currently the most successful smoking cessation pharmacotherapy (12, 13). Initial studies suggested an $(\alpha4)_2(\beta2)_3$ subunit stoichiometry for these nAChR (18, 19). However, more recent work indicates that both native and heterologously expressed α4β2-nAChR can exist in two isoforms with $(\alpha4)_2(\beta2)_3$ and $(\alpha4)_3(\beta2)_2$ subunit stoichiometries, respectively, displaying high and (predominantly) low sensitivities (HS and LS) to activation by acetylcholine (ACh) (20–25). The expression of α4β2-nAChR isoforms appears to be physiologically significant. For example, multiple epilepsy-associated α4 and β2 subunit mutants alter ratios of HS to LS α4β2-nAChR isoforms (17, 26), and agonists capable of preferentially stimulating LS α4β2-nAChR produce distinctive physiological effects (27–29). Accordingly, a better understanding of the respective roles of HS and LS α4β2*-nAChR isoforms is likely to have considerable translational implications.

Agonist binding to nAChR is primarily driven by interactions with a set of six peptide loops located at subunit interfaces. Three (loops A–C) are contributed from the subunit on the principal or (+)-side of the interface, with the remaining three (loops D–F) being contributed from the subunit on the complementary or (−)-side of the interface. The (−)-side subunit is oriented counterclockwise from the (+)-side subunit when viewed from extracellular space (Fig. 1*A*) (20). A high degree of conservation of critical agonist binding residues is seen across

* This work was supported by National Institutes of Health Grants DA026627 and DA012242 (to P. W.) and DA030929 (to J. M. L.) and by endowment and capitalization funds from the Men's and Women's Boards of the Barrow Neurological Foundation (to P. W. and R. J. L.). The authors declare that they have no conflicts of interest with the contents of this article. The content is solely the responsibility of the authors and does not necessarily represent the official views of the National Institutes of Health.

[1] To whom correspondence should be addressed: Division of Neurobiology, Barrow Neurological Institute, 350 W. Thomas Rd., Phoenix, AZ 85013. Tel.: 602-406-6534; Fax: 602-406-4172; E-mail: paul.whiteaker@dignityhealth.org.

[2] The abbreviations used are: nAChR, nicotinic acetylcholine receptor; ACh, acetylcholine; CRC, concentration response curve; HS, high sensitivity; HSP, high sensitivity (pentameric concatemer); LS, low sensitivity; LS(P), low sensitivity (pentameric concatemer); ANOVA, analysis of variance.

subunits. This includes residues within interfaces that do not harbor conventionally recognized canonical α(+)/(−)β-type agonist binding pockets (30–34). Both α4β2-nAChR isoforms host a pair of canonical orthosteric, high affinity α4(+)/(−)β2 agonist binding interfaces, but the LS $(\alpha4)_3(\beta2)_2$ -nAChR isoform also contains a unique, non-canonical, α4(+)/(−)α4 agonist-binding site (34–36). This α4(+)/(−)α4 site has lower affinity for ACh or nicotine than the α4(+)/(−)β2 site, making it responsible for the intrinsically biphasic ACh concentration-response profile of the LS $(\alpha4)_3(\beta2)_2$-nAChR isoform. This complex CRC distinguishes it from the HS $(\alpha4)_2(\beta2)_3$-nAChR isoform, which lacks an α4(+)/(−)α4 subunit interface and produces monophasic CRCs (34–36).

Activation of LS α4β2-nAChR via interactions with a sufficiently high agonist concentration to engage all three binding sites confers large increases in per receptor function compared with the HS isoform α4β2-nAChR, which can only be activated by agonist binding at the common pair of α4(+)/(−)β2 sites (36). Importantly, activation of the HS phase of functional responsiveness by LS $(\alpha4)_3(\beta2)_2$-nAChR can occur just by targeting the common pair of α4(+)/(−)β2 sites (either at agonist concentrations too low to engage the α4(+)/(−)α4 site or by highly selective agonists that do not engage the α4(+)/(−)α4 site at all). In this case, function per receptor closely resembles that of the HS $(\alpha4)_2(\beta2)_3$-nAChR isoform (34, 36, 37). Although the α4(+)/(−)α4 interface retains the typical features of an nAChR agonist-binding site, it may therefore be thought of as effectively potentiating the response as would a co-agonist or positive allosteric modulator site (34–36). These previous studies by ourselves and others have implicitly treated the two canonical α4(+)/(−)β2 agonist-binding sites as a functionally equivalent pair. However, as illustrated in Fig. 1*A*, the nAChR pentameric assemblies of each isoform are pseudosymmetrical; the subunits that contribute the α4(+)/(−)β2 agonist-binding sites are surrounded by different neighbors. Because of this, it seemed possible that the two canonical agonist-binding sites might contribute differentially to activation (both within each isoform and between the two isoforms).

To test this hypothesis, we used a concatemeric (linked subunit) nAChR approach. This allowed us to express pure populations of both HS and LS isoform α4β2*-nAChR and to systematically mutate agonist-binding residues of α4(+)/(−)β2 interfaces either individually or in combinations on either background (Fig. 1). Unlike our previous study (36), we wished to modify, not destroy, ligand binding at the targeted sites. Therefore, we systematically altered triplets of β2 subunit (−)-face E-loop residues to their non-conserved counterparts in the α4 subunit (β2(V136H,F144Q,L146T); β2HQT) (Fig. 1*B*). This can convert agonist binding at α4(+)/(−)β2 sites to closely resemble that at an α4(+)/(−)α4 agonist-binding site (34, 38). If our hypothesis is correct, then making equivalent E-loop modifications in nominally equivalent α4(+)/(−)β2 interfaces should produce different outcomes. We also reciprocally mutated α4 subunit (−)-face E-loop residues (α4(H142V, Q150F,T152L); α4VFL (34)) to examine the effects of this substitution inside, outside, or in the absence of an α4(+)/(−)α4 interface, on both HS and LS backbones (Fig. 1*C*).

We demonstrate that the contributions of α4(+)/(−)β2 agonist-binding sites differ substantially within the HS isoform and between the two different isoforms upon β2HQT substitution. We further demonstrate that, unexpectedly, the α4VFL mutation produces very similar functional changes whether it is inserted into the LS isoform-unique α4(+)/(−)α4 agonist-binding site or not. Evidence for other allosteric effects of subunit (−)-face, E-loop, alterations also is obtained. These new insights may provide further opportunities to develop compounds that pharmacologically distinguish between the isoforms and thus increase our understanding of each isoform's role in normal and disease physiology.

Experimental Procedures

Chemicals—Sazetidine-A and A-85380 were kindly provided by Drs. Alan Kozikowski (University of Illinois, Chicago) and F. Ivy Carroll (Research Triangle Institute, Research Triangle Park, NC), respectively. All other reagents were purchased from Sigma, unless noted otherwise.

Preparation of Unlinked α4β2-nAChR Wild-type and Triple Mutant E-loop cDNA Constructs—Unlinked nAChR human wild-type (WT) α4 (*CHRNA4*; NCBI reference sequence designation NM_000744.6) or β2 (*CHRNB2*; NM_000748.2) subunit cDNAs were transcriptionally optimized, synthesized, and sequenced by GeneArt (ThermoFisher Scientific, Inc., Waltham, MA). Each subunit was subsequently excised from the GeneArt shuttle vector with the restriction enzymes XbaI and NotI and subcloned into a modified pCI expression vector containing an SwaI linearization site (vector was a gift from Dr. Isabel Bermudez, Oxford Brookes University, Oxford, UK). The unlinked triple mutant α4(H142V,Q150F,T152L) (α4VFL) or β2(V136H,F144Q,L146T) (β2HQT) subunit cDNAs were also synthesized and sequenced by GeneArt as variants of their optimized WT parent subunits. These mutants were then subcloned into pCI as described previously.

Preparation of Concatemeric α4β2-nAChR cDNA Constructs Containing Wild-type and Triple Mutant E-loop Subunits—Dr. Isabel Bermudez (Oxford Brookes University) provided a low sensitivity pentameric (LSP) α4β2-nAChR construct encoding concatenated human nAChR subunits in the order β2-α4-β2-α4-α4 (21). This construct, cloned into the previously mentioned modified pCI expression vector, served as the parent plasmid for each of the concatemers engineered for this study. This included the high sensitivity pentameric isoform (β2-α4-β2-α4-β2; HSP) α4β2-nAChR construct (Fig. 1). The basic construction strategy has been described in detail elsewhere (21, 36). Briefly, all but the first β2 subunit were absent their start codons and signal peptides, and all but the last were devoid of a stop codon. Each subunit was tethered to its neighbor by a short stretch of nucleotides encoding a series of 6 or 9 $(\text{Ala-Gly Ser})_n$ repeats, engineered to ensure a total linker length (including the C-terminal tail of the preceding subunit) of 40 ± 2 amino acids. A unique set of six restriction sites either flanking the entire concatemer or approximately bisecting each linker between subunits was introduced along the pentamer sequence (Fig. 1*A*). This permitted replacement of individual subunits (or cassettes of multiple subunits if desired) using standard restriction digestion and ligation methods. GeneArt was used to

design, synthesize, and sequence-verify optimized WT and mutant subunits for substitution into the parent construct. These new subunits were variants of the unlinked optimized subunits previously described, with the addition of the flanking AGS-repeat linkers and restriction sites required for correct placement within the resulting new pentameric concatemers. A unique restriction site was also introduced into each synthetic mutant sequence destined for ligation within a concatemer. This allowed for unambiguous verification of every new construct.

RNA Preparation and Oocyte Injection—As described previously (36), both unlinked and concatenated plasmid cDNA constructs were SwaI-linearized, proteinase K-treated, column-purified, and transcribed into cRNA (mMessage mMachine T7 kit, Ambion, ThermoFisher Scientific, Waltham, MA). Each cRNA sample was DNase I-treated, column-cleaned, and gel-analyzed for size and quality. Stage V/VI *Xenopus laevis* oocytes, purchased from Ecocyte LLC (Austin, TX), were injected with biased ratio combinations of mRNAs encoding unlinked subunits (1 or 10 ng) or with 20 ng of mRNA encoding a concatemeric construct. Injected oocytes were incubated at 13 °C for 6–10 days before testing.

Two-electrode Voltage Clamp Electrophysiology—Methodology for obtaining CRCs and maximal current responses from nAChR-injected oocytes has been published elsewhere (36, 39, 40). Briefly, at least 6 days post-injection, oocytes were voltage-clamped at −70 mV with an Axoclamp 900A amplifier (Molecular Devices, Sunnyvale, CA). Recordings were sampled at 10 kHz (low pass Bessel filter, 40 Hz; high pass filter, direct current), and the traces were extracted and analyzed using Clampfit software (Molecular Devices). Any oocytes with leak currents >50 nA were discarded. Drugs were applied at a flow rate of 4 ml min^{-1} using a 16-channel, gravity-fed perfusion system with automated valve control (AutoMate Scientific, Inc., Berkeley, CA) in OR2 buffer (NaCl, 82.5 mM; KCl, 2.5 mM; $MgCl_2$, 1 mM, HEPES 5 mM, pH 7.6) at 22 °C. Solutions were supplemented with atropine sulfate (1.5 μM) to block any muscarinic responses. Agonists were acutely perfused for 1 s with a 60-s washout between drug applications. In CRC analyses requiring a 5-min sazetidine-A (3.16 nM) pretreatment, both ACh and wash applications contained the same concentration of sazetidine-A. All concentration-response recording sessions included oocytes injected with non-mutant HSP and LSP concatemer controls (minimum of three oocytes per group) to account for day-to-day and batch-to-batch variability in functional expression levels.

^{125}I-mAb 295 Labeling of X. laevis Oocyte Surface nAChR Populations—Introduction of any mutation could potentially alter surface expression of the host nAChR. Any such changes would have corresponding effects on functional expression, independent of effects on function per receptor. Surface expression levels of each concatenated α4β2-nAChR isoform, and variant thereof, were quantified with ^{125}I-mAb 295 in an oocyte binding assay. For consistency, the entire family of either LSP or HSP triple E-loop mutants was tested on the same day. LSP and HSP controls (containing no E-loop mutant subunits) were included in every experiment. mAb 295 is a monoclonal antibody that specifically recognizes correctly folded human, bovine, and rodent nAChR β2 subunits (41–43). The protocol used has previously been described (26, 36, 44). In brief, following determination of expressed nAChR function by maximal stimulation (I_{max}, where I_{max} is peak current response) with ACh (EC_{100}, 1 s), sets of six oocytes each expressing individual concatemeric α4β2-nAChR isoforms or variants thereof were sorted into a 24-well plate (one set per well). The accompanying OR2 buffer was aspirated from each well and replaced with 2 nM ^{125}I-mAb 295 in OR2 (200 μl), supplemented with 10% heat-inactivated fetal bovine serum (to reduce nonspecific binding), and incubated with gentle agitation for 3 h at 22 °C. Washing was performed by aspiration of the radioactive solution and replacement with OR2 supplemented with 10% heat-inactivated fetal bovine serum (2 ml, ice-cold). The oocytes were then transferred to a fresh 24-well plate with the minimum possible volume of diluted radioactive solution. This wash protocol was repeated twice more. The thrice-washed oocytes were transferred to another fresh 24-well plate before being lysed overnight in 0.1% SDS, 0.01 N NaOH (0.5 ml), prior to scintillation counting at 85% efficiency using a Packard TriCarb 1900 Liquid Scintillation Analyzer (PerkinElmer Life Sciences). One or more wells of non-injected oocyte controls were included per assay plate to determine nonspecific binding. Nonspecific binding was subtracted from total binding determined in each of the other wells of the same plate, to calculate specific binding. Mean specific counts for sets of six HSP or LSP isoform-expressing oocytes were 885 and 469 cpm, respectively. This compared with mean nonspecific binding of 98 cpm per set of six uninjected oocytes. Specific cell-surface binding of ^{125}I-mAb 295 was converted to nAChR surface expression per oocyte using the specific activity of the radioligand (initially 1150 Ci/mmol, but falling due to non-catastrophic decay of the radiolabel) and by accounting for two antibody-binding sites (two β2 subunits) per LSP isoform variant or three binding sites (three β2 subunits) per HSP variant (Fig. 1). For each experiment, the resulting binding data (femtomoles of nAChR/oocyte) were used to normalize I_{max} values (microamperes/oocyte; calculated as the mean of the individually measured I_{max} values obtained from the oocytes comprising the set of six used in each binding determination) to microampere/fmol. These specific function values were then compared among all E-loop mutant concatemers and to the non-E-loop mutant LSP and HSP controls.

Data Analysis—Log_{10} EC_{50} values were determined from individual CRCs by non-linear least squares curve fitting (Prism 5.0; GraphPad Software, Inc., La Jolla, CA). Unconstrained monophasic or biphasic logistic equations were used to fit all parameters, including Hill slopes and fractional contributions of function attributable to HS or LS nAChR, where applicable. A sum-of-squares *F*-test was used to verify when data were better fit by the biphasic rather than monophasic model. Note that precision in determining ACh log_{10} EC_{50} values from biphasic CRCs (S.E. in log_{10} EC_{50} values between 0.1 and 0.35) is substantially lower than for monophasic CRCs (log_{10} EC_{50} S.E. values ≤0.07). One-way analysis of variance (ANOVA) and Bonferroni's multiple comparison tests were used to compare functional parameters across α4β2-nAChR variants (Prism 5.0 or SigmaPlot Version 12.5, Systat Software Inc., San Jose, CA).

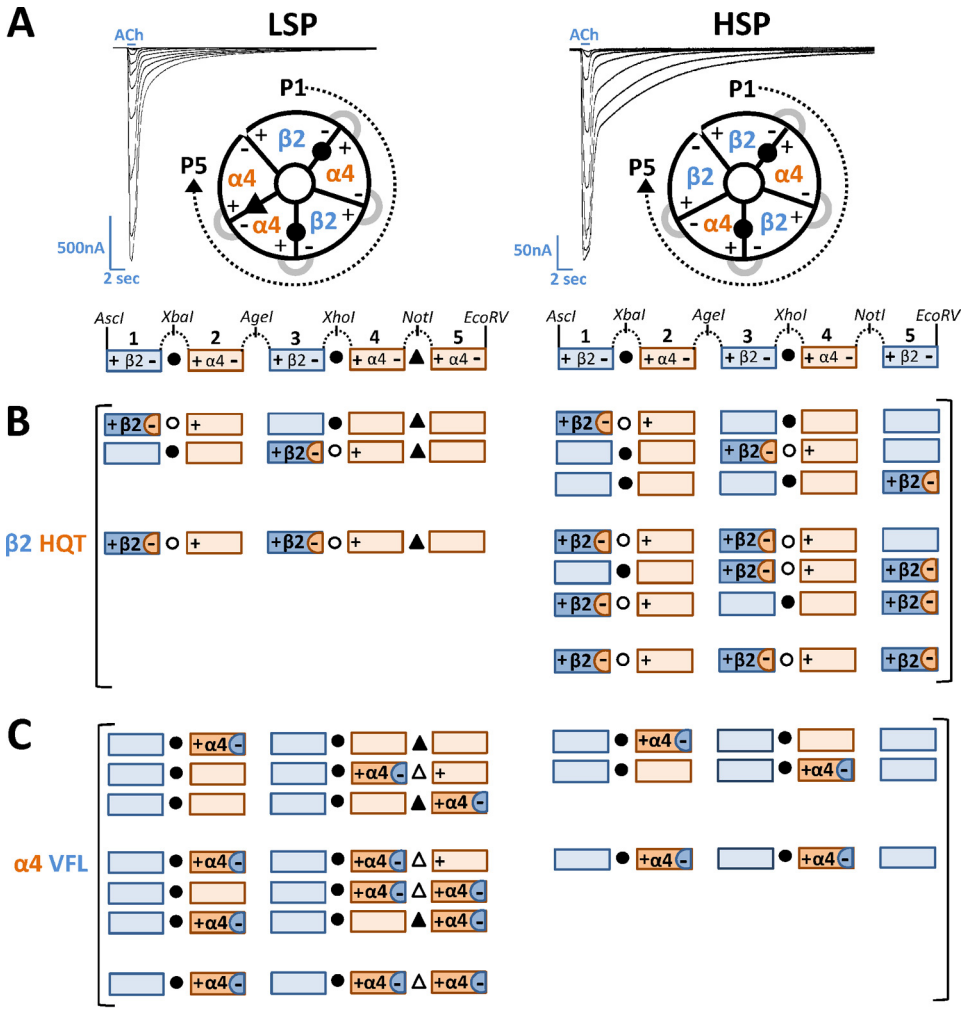

FIGURE 1. **Schematic illustration of E-loop chimera construction using concatenated LS $(\alpha4)_3(\beta2)_2$ and HS $(\alpha4)_2(\beta2)_3$ isoforms of nAChR.** *A, top,* diagram representing the linked LSP and HSP α4β2-nAChR isoforms. Illustrated are subunit positions and agonist binding pockets (*filled circles* and *triangle*) formed from a principal (+) and E-loop-containing complementary (−)-face as observed from extracellular space. This convention is used in subsequent figure captions to indicate the positions of agonist binding pockets within parent constructs for concatemer series harboring one or more mutant subunits. Also shown are typical responses to a range of ACh concentrations for these two isoforms (LSP $10^{-7.5}$ to 10^{-4} M; HSP $10^{-7.5}$ to 10^{-5} M), performed on day 6 post-injection. Traces for mutant variants of these two parent constructs showed very similar waveforms, other than in terms of peak current magnitude. *Bottom*, at the cDNA level, individual subunits within the LSP or HSP backbone are tethered by linkers encoding AGS repeats. Linkers are bisected by unique restriction sites that allow rapid substitution of one or more E-loop mutant-containing counterparts. *B,* a series of 10 concatemers was constructed from either the LSP (*left panel*) or HSP (*right panel*) WT parent by cloning one, two, or three copies of the β2 subunit hosting the non-identical α4-equivalent E-loop residues H136Q144T146 (β2HQT (34)). Each mutant β2 subunit is highlighted in *dark blue* and *boldface* with the chimeric α4 E-loop-containing (−)-face depicted by an *orange semicircle*. Note that *open symbols* represent altered ligand-binding sites. *C,* 10 additional concatemers were constructed with the reciprocal β2 E-loop residues placed in one, two, or three copies of α4 subunits. The V142F150L152 (α4VFL**)** subunit is labeled and arranged as in *B* using contrasting colors.

Results

Acetylcholine Concentration-Response Curves Generated from the β2HQT Chimeric E-loop Subunit Introduced into Either LS- or HS-based α4β2-nAChR Concatemers Reveal Position-, Copy-, and Isoform-specific Effects—As noted in the Introduction, the account describing how HS phase function arises in either LS or HS isoform α4β2-nAChR (34, 36) contains an implicit assumption. This is that the two α4(+)/(−)β2 agonist-binding sites found in both isoforms (see Fig. 1*A*) are functionally equivalent (both to each other in a given pentameric backbone, and between HS and LS α4β2-nAChR isoforms). Fully linked pentameric constructs provide the ability to substitute E-loop mutant subunits at any chosen position or combination of positions in HS or LS isoform α4β2-nAChR. Using these concatemeric constructs, we were therefore able to systematically test this assumption for the first time, by introducing the β2HQT E-loop mutant (located on the (−)-side of the β2 subunit) into defined positions within LSP and HSP α4β2-nAChR (Fig. 1*B*). The resulting family of constructs represents every possible permutation of the β2HQT triple mutant subunit cloned into the WT LSP and HSP parent constructs.

In the case of the LSP-based constructs, substitution of the (−)α4-like β2HQT mutant subunit into either of the α4(+)/(−)β2 agonist-binding sites (transforming the interface into something resembling the lower affinity α4(+)/(−)α4 interface) abolished HS component function (Fig. 2*A*). The same was true when β2HQT substitution was performed at both α4(+)/(−)β2 sites. The resulting monophasic CRCs produced by the three mutant LSP constructs had very similar $\log_{10}$ EC_{50} values to each other (EC_{50} ≈230 μM) and were approximately

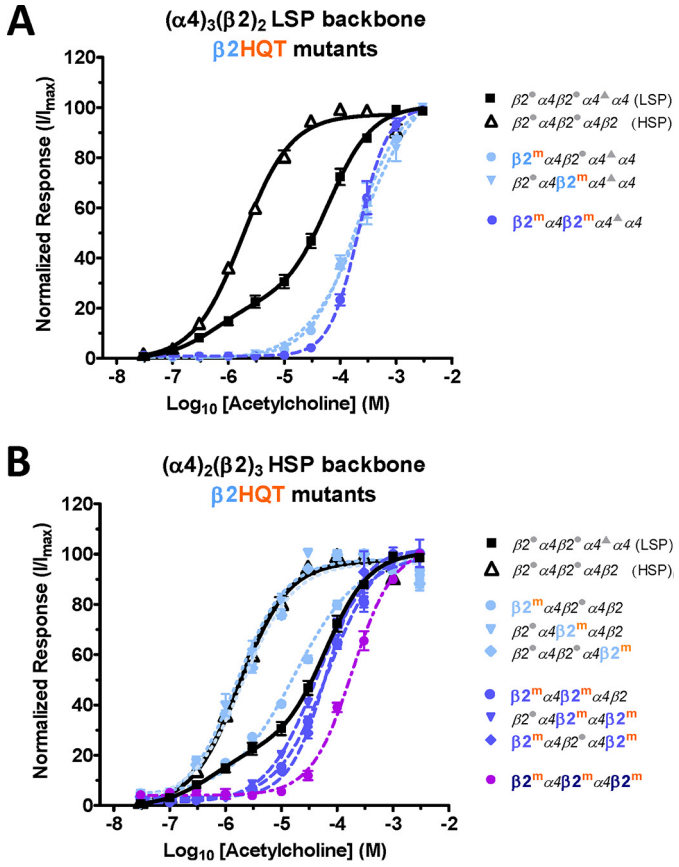

FIGURE 2. **ACh concentration-response profiles for the β2HQT E-loop mutant series of concatenated LS and HS α4β2-nAChR isoforms.** *A,* oocytes expressing concatenated LSP constructs incorporating one or two copies of the β2HQT E-loop mutant subunit (position(s) indicated by $\beta2^m$) were acutely stimulated with the indicated range of ACh concentrations. All three mutant concatemers generated similar monophasic CRCs lacking the HS component seen in WT LSP. *B,* seven-member HSP family of β2HQT E-loop mutant concatemers generated three classes of CRCs ranging from no ACh affinity change for single copy position 3 or 5 constructs to a biphasic response for single copy position 1 and finally to LS-like for each of the double and triple copy versions. Choice of fitting each CRC to either a one- or two-site unconstrained logistic model was made using the extra sum-of-squares *F*-test. Details of the obtained pharmacological parameters and the statistical analysis used to compare results are provided in Table 1. Data points represent the mean (±S.E.) of at least four oocytes (numbers provided in Table 1). CRCs obtained using wild-type LSP (■) and HSP (△) parent constructs are included in both graphs for ease of comparison within and between isoforms.

TABLE 1

Effects of introducing β2HQT E-loop mutant subunits into the LSP and HSP α4β2 nAChR concatemer backgrounds (ACh CRCs)

Oocytes were injected with RNA encoding concatenated LSP or HSP α4β2-nAChR constructs containing zero (LSP or HSP controls in boldface), one, or more copies of the β2HQT subunit at the position (s) shown in blue type. TEVC recording of agonist perfused oocytes was used to establish ACh CRCs (Fig. 2, "Experimental Procedures"). Least squares curve fitting was used to determine ACh $\log_{10}$ (M) ± S.E. values. Data were fit to an unconstrained monophasic logistic model, unless data were better fit to a biphasic logistic model (determined using the extra sum-ofsquares *F*-test). For biphasic fits, ACh $\log_{10}$ (M) EC_{50} ± S.E. values were estimated for both LS and HS phases, and the fractional HS component of the biphasic response also was estimated. The number of individual oocytes is designated (*n*; typically for 2–4 oocytes per individual test). Since data were collected on a single day for the complete set of mutants on either the LSP or HSP backbone (see "Experimental Procedures"), including all β2HQT and α4VFL mutant constructs, one-way ANOVA was applied to determine significant differences between all $\log_{10}$ EC_{50} values collected on the LSP backbone, and a second analysis was performed on the full set of $\log_{10}$ EC_{50} values collected on the HSP backbone. In addition, data representing ACh-activated maximal function (I_{max} in nA, rounded to 1 or 2 significant digits) and I_{max} values corrected for surface nAChR (microampere/fmol) were generated from (*N*) experiments testing 6 individual oocytes per concatemer per experiment (See Figs. 4 and 5 for these data shown relative to and compared with those derived from control LSP and HSP concatemers, respectively). All current amplitude-based data are means ± S.E.

Concatemer	*ACh (Log_{10} M) EC_{50}(HS)*	*ACh (Log_{10} M) EC_{50}(LS)*	*HS Fraction*	*n*	*ACh I_{max} (nA)*	*μA/fmol*	*N*
β2α4β2α4α4 (LSP)	**-6.25 ± 0.35**	**-4.20 ± 0.10†††**	**0.23 ± 0.12[a]**	**10**	**3900 ± 260**	**194.6 ± 33.8**	**7**
β2α4β2α4α4		-3.70 ± 0.04†††	*lost*	4	1100 ± 120	364.5 ± 182.9	6
β2α4β2α4α4		-3.59 ± 0.07†††	*lost*	4	3500 ± 260	415.1 ± 182.4	6
β2α4β2α4α4		-3.67 ± 0.03†††	*lost*	4	830 ± 80	150.7 ± 26.0	5
β2α4β2α4β2 (HSP)	**-5.75 ± 0.03**			**11**	**500 ± 40**	**19.3 ± 4.7**	**4**
β2α4β2α4β2	-5.56 ± 0.45	-4.23 ± 0.15***	0.51 ± 0.26[b]	9	60 ± 10	8.4 ± 1.4	3
β2α4β2α4β2	-5.81 ± 0.06			4	1300 ± 150	44.1 ± 10.2	4
β2α4β2α4β2	-5.69 ± 0.05			4	700 ± 90	29.0 ± 9.2	4
β2α4β2α4β2		-4.17 ± 0.04***		4	80 ± 10	17.6 ± 1.9	4
β2α4β2α4β2		-4.39 ± 0.04***		8	500 ± 60	27.3 ± 4.9	4
β2α4β2α4β2		-4.19 ± 0.04***		4	30 ± 3	2.3 ± 1.1	4
β2α4β2α4β2		-3.73 ± 0.03***		4	60 ± 7	7.4 ± 0.9	3

††† One-way ANOVA determined significant differences among the $\log_{10}$ EC_{50} values derived from LSP background CRC data (including those measured for the biphasic response of the unmodified LSP control construct; $F_{12,63} = 21.29$, $p < 0.0001$). Post hoc comparisons were performed using the Bonferroni correction, and showed that the low-sensitivity phase of un-modified (control) LSP responses had an $\log_{10}$ EC_{50} value significantly different to that of the control high-sensitivity phase response of the same construct. Further, the $\log_{10}$ EC_{50} values of the monophasic responses of all three LSP β2HQT mutant constructs were also significantly different from that of the HS-phase control response, but indistinguishable from each other and that of the low-sensitivity phase response of the control construct: the difference of this group of LS-like responses from the control HS-phase response is denoted as †, $p < 0.001$.

*** One-way ANOVA identified significant differences across the $\log_{10}$ EC_{50} values calculated from the HSP-background CRCs (including that obtained from the unmodified HSP control construct; $F_{14,92} = 17.33$, $p < 0.0001$). Post hoc comparisons were performed using the Bonferroni correction and again showed that the $\log_{10}$ EC_{50} values could be divided into two groups (one indistinguishable from that of the monophasic HS phase response of the non-mutant HSP control, and a second with significantly lower ACh potency; all values in the LS phase group were statistically indistinguishable from each other). The difference of the LS-like group $\log_{10}$ EC_{50} values from those of the HS-like group is noted as ***, $p < 0.001$. Extra sum-of-squares *F* test for a biphasic model preferred over a monophasic model: [a], $F_{(DFn = 6,DFd = 100)} = 19.95$; $p < 0.0001$; [b], $F_{(DFn = 3,DFd = 86)} = 19.95$; $p < 0.0003$.

one-half log unit higher than the estimated $\log_{10}$ EC_{50} value for the LS component of LSP control (EC_{50} ≈60 μM; Fig. 2*A*, Table 1). In summary, β2HQT substitution effects on α4β2-nAChR LSP isoform function were both position- and copy number-independent; in every case the resulting function was purely LS component-like.

In striking contrast to the LSP series, the HSP-derived family of β2HQT-containing concatemers generated a complex set of CRCs that could be classified into three groups (Fig. 2*B*). The first group consisted of two concatemers hosting a single copy of β2HQT at positions 3 or 5, which yielded HS $\log_{10}$ EC_{50} values indistinguishable from that of the unmutated HSP control (EC_{50} ≈2 μM; Table 1). Note that the β2HQT subunit in position 3 is part of an α4(+)/(−)β2 binding pocket, although that in position 5 is not (Fig. 1*B*). In other words, these constructs had one (β2HQTp3) or no (β2HQTp5) α4/β2 interfaces converted to a mock α4(+)/(−)α4 interface, retaining one or both natural α4(+)/(−)β2 interfaces, respectively.

The second HSP mutant group had just one member, the HSP concatemer containing a single β2HQT subunit at position 1. This β2HQTp1 construct also had one α4(+)/(−)β2-to-mock α4(+)/(−)α4 interface conversion but, like the β2HQTp3 mutant, preserved one α4(+)/(−)β2 interface. This concatemer was the only HSP β2HQT mutant construct that generated a biphasic ACh CRC. The observed HS and LS phase EC_{50} values for this construct (≈1.8 and ≈60 μM, respectively) were indistinguishable from those of the LSP control (≈2.8 and ≈60 μM; Table 1). This biphasic response was so striking that it was further confirmed using two highly HS *versus* LS isoform-selective nicotinic agonists, A-85380 and the structurally

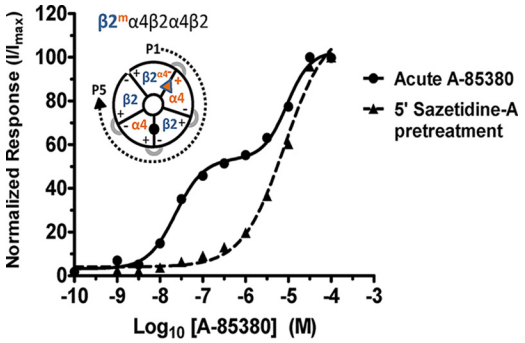

FIGURE 3. **Sazetidine-A pretreatment abolishes HS component function in oocytes expressing the β2HQT position 1 HSP concatemer.** Acute responses to the indicated range of A-85380 concentrations were measured before and after a 5-min pretreatment with 3.16 nM sazetidine-A in the β2HQT position 1 HSP concatemer. Without pretreatment, despite mutating one of the canonical α4(+)/(−)β2 interfaces, a significant fraction of HS function was retained in this construct. A-85380 generated a strongly biphasic CRC ($\log_{10}$ EC_{50} HS = −7.64 ± 0.04, $\log_{10}$ EC_{50} LS = −5.04 ± 0.04, and fractional HS contribution = 0.51 ± 0.02). This CRC became monophasic (LS-only) following a desensitizing treatment with sazetidine-A ($\log_{10}$ EC_{50} = −5.09 ± 0.05). n = 4 oocytes per treatment. Note the *inset* that shows the location of the subunits carrying the mock α4(+)/(−)α4 interface surrounded by WT β2 neighbors which, among all of the mutant constructs generated in this study, uniquely mimics the structure of the unmutated LSP construct.

related compound sazetidine-A. A-85380 demonstrates an unusually high degree of agonist selectivity between HS and LS isoform α4β2-nAChR (24, 36, 45). In response to acute A-85380 stimulation, the HSP β2HQT position 1 construct generated a clearly biphasic CRC with an ~1:1 distribution of HS and LS components (Fig. 3), confirming the initial observation of a biphasic ACh CRC. Sazetidine-A (46) activates only HS isoform α4β2-nAChR with high efficacy (47) and may be used to selectively occupy (36, 37) and inactivate (by desensitization) responses arising from α4(+)/(−)β2 interfaces (36). A desensitizing concentration of sazetidine-A (3.16 nM (36)) was used to pretreat oocytes expressing the HSP β2HQT position 1 concatemer prior to acute A-85380 exposure. This led to complete suppression of the HS portion of the response, confirming that the resulting CRC must arise from A-85380 activity at the remaining ((position 4) α4(+)/(−)β2 (position 3)) interface left within the position 1 HSP β2HQT construct.

The third group of HSP mutants consisted of all concatemers containing two copies of the β2HQT E-loop, plus that with all three positions mutated to the β2HQT (Fig. 2*B* and Table 1). All three doubly substituted constructs produced $\log_{10}$ EC_{50} values indistinguishable from each other or from that of the LS phase of unmutated LSP α4β2-nAChR (EC_{50} ≈60 μM). Interestingly, even a combination of β2HQT subunits placed in positions 3 and 5 (neither of which had any effect individually) resulted in loss of all HS phase function. The EC_{50} value for the triple β2HQT mutant HSP (≈190 μM) was like that of β2HQT mutants introduced into the LSP backbone (Fig. 2*A* and Table 1). Thus, in complete contrast to the effects of β2HQT mutant subunit incorporation on LSP α4β2-nAChR, effects in HSP α4β2-nAChR constructs were strongly influenced both by position and by copy number. Most importantly, effects on ACh CRC responses were radically different between the two constructs in which a single β2HQT mutant subunit was placed in either of the two nominally identical α4(+)/(−)β2 agonist binding pockets.

ACh-induced Function Per Surface-expressed LS or HS α4β2-nAChR Concatemer Reveals Position-, Copy-, and Isoform-specific Effects of β2HQT Chimeric E-loops—In addition to exploring effects of β2HQT substitution at defined subunit positions on agonist activation affinities, we also wanted to assess effects on amounts of nAChR function. We previously have shown that cell surface levels of HSP and LSP α4β2-nAChR isoforms in oocytes injected with equivalent levels of pentamer cRNA are comparable (36). This indicated that the observed differences in amount of HSP *versus* LSP function were almost exclusively due to differences in function per surface-expressed nAChR; *i.e.* due to the intrinsic properties of the α4β2-nAChR isoforms. We have also shown that introducing mutations at subunit interfaces can significantly affect surface expression of the resulting nAChR constructs (36). Accordingly, we normalized function to the amount of nAChR surface expression (measured using β2-specific monoclonal antibody binding).

For the LSP β2HQT mutant constructs, measurements of maximum ACh-induced function (I_{max}) alone showed significant losses of function for both the position 1-only and double mutant β2HQT mutant constructs, reducing I_{max} to a level resembling that of the unmutated HSP control construct (Fig. 4*A*). The LSP position 3-only β2HQT mutant construct, in contrast, produced an unchanged I_{max} value compared with the unmutated LSP construct. However, as shown in Fig. 4*B*, surface expression of all three LSP β2HQT mutant constructs was significantly suppressed by incorporation of the mutant subunit(s). When we compensated for this effect (Fig. 4*C*), it became apparent that function of both single mutant LSP β2HQT mutant constructs was significantly increased, to approximately double that of the unmutated LSP control, on a per nAChR basis (Table 1). Also, on a per nAChR basis, function of the position 1 + 3 double LSP β2HQT mutant construct was statistically similar to that of the unmutated LSP α4β2-nAChR construct (Fig. 4*C* and Table 1). As in the case of $\log_{10}$ EC_{50} values (Fig. 2*A*), β2HQT-mediated functional enhancement in LSP was position-independent. However, copy number did affect the per nAChR amount of function, unlike effects on agonist $\log_{10}$ EC_{50} values that were the same regardless of whether one or both positions contained β2HQT mutant subunits (Fig. 2*A*).

The family of HSP β2HQT concatemers again revealed a more complicated response to incorporation of mutant subunits (Fig. 5 and Table 1). The single copy β2HQT position 1 construct (the only α4β2 HSP mutant to produce a biphasic CRC; Fig. 2*B*) exhibited significantly lower surface expression and I_{max}. On a per nAChR basis, these effects combined to produce an apparent, but not-quite-significant, reduction in per nAChR function. In contrast, the position 3-only β2HQT mutant (which did not affect the ACh concentration-response outcome; Fig. 2*B*) significantly increased I_{max} compared with the unmutated HSP control, while having no effect on surface expression. On a per nAChR basis, this resulted in a statistically significant doubling of function. Although the non-agonist-binding interface position 5 β2HQT single mutant HSP construct showed a modest but marginally significant increase in I_{max} compared with the non-mutant HSP control, this did not quite retain significance on a per nAChR basis. Neither did this

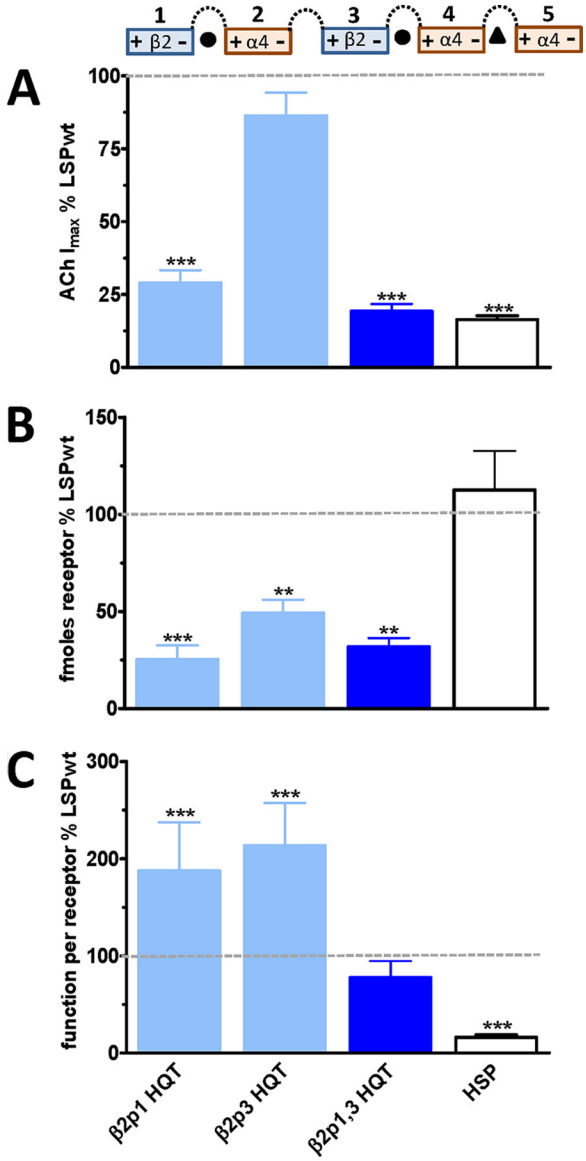

FIGURE 4. **β2HQT E-loop mutation effects on peak ACh-induced function (I_{max}) and nAChR surface expression within LSP concatemers.** Oocytes expressing concatenated LSP constructs incorporating one or two copies of the β2HQT E-loop mutant subunit were screened for maximal ACh current responses, followed by ^{125}I-mAb 295 binding to determine femtomoles of surface nAChR (assuming two β2-binding sites per LSP and three per HSP construct, see "Experimental Procedures"). All results, including the WT HSP control, were normalized to the unmutated LSP concatemer for at least four individual experiments (denoted with a *dashed horizontal line* in each panel; see Table 1 for non-normalized data and number of replicates/experiments performed). *A*, I_{max} was reduced ~4-fold (close to HSP levels) for the LSP constructs harboring β2HQT mutations in position 1 or positions 1 + 3, although the position 3 variant was unchanged. *B*, surface nAChR expression levels were reduced 50–75% across all three LSP β2HQT mutant constructs. Note that the unmutated HSP construct had a similar level of surface expression as that of the unmutated LSP construct, confirming our earlier finding (36). *C*, I_{max} values were normalized to amounts of nAChR surface expression for each LSP β2HQT mutant concatemer. Function per surface nAChR was increased ~2-fold for each of the single position LSP mutants, whereas the double position variant had WT levels of function. HSP typically produced ~10% of LSP-mediated function per receptor in this study. Because data were collected for the complete set of mutants on the LSP backbone in each individual experiment (see "Experimental Procedures"), including all β2HQT and α4VFL mutant constructs, one-way ANOVA was applied to determine significant differences within the sets of I_{max}, surface expression, or function per receptor values collected on the LSP backbone. One-way ANOVA determined that significant differences existed between LSP backbone groups in each panel as follows: *A*, $F_{12,77} = 57.23$; $p < 0.001$; *B*, $F_{12,63} = 5.69$; $p < 0.001$; *C*, $F_{12,63} = 36.56$; $p < 0.001$. Post hoc comparisons were performed in each case using the Bonferroni correction; differences from the unmutated LSP control are noted as follows: **, $p < 0.01$; ***, $p < 0.001$.

position 5-only mutant construct produce any effect on ACh concentration-response (Fig. 2*B*). Interestingly, per nAChR function of two of the HSP double-β2HQT mutant constructs (positions 1 + 3 and 3 + 5) did not significantly differ from that of HSP control. However, when the position 1 β2HQT subunit was included with the off-interface position 5 β2HQT subunit, in either the double and triple mutant configurations (*e.g.* positions 1 + 5, or positions 1 + 3+5), there was a highly significant, ≥60%, reduction in function per nAChR. To summarize, position- and copy-dependent β2HQT mutant subunit effects on per nAChR function again exposed asymmetries between the nominally similar α4(+)/(−)β2-binding sites within the HSP α4β2-nAChR isoform.

Acetylcholine Concentration-Response Curves and per nAChR Function of LS and HS nAChR Concatemers Reveal Symmetrical and Copy-dependent Effects of α4VFL Chimeric E-loop Subunit Introduction—In addition to the just-explored α4(+)/(−)β2 agonist-binding sites common to HSP and LSP α4β2-nAChR, we also wished to specifically target the unique α4(+)/(−)α4 interface present between positions 4 and 5 within the LSP (Fig. 1*A*, *left panel*). A previous study (34) had addressed this question using unlinked α4VFL mutant subunits. However, the unlinked subunit approach altered all three α4 subunits in the α4β2-nAChR LS isoform. In contrast, use of concatemeric constructs allowed us to assess effects of α4VFL mutant incorporation at each available position, either singly or in combination (see Fig. 1*C*).

Unexpectedly, CRCs obtained from the family of α4β2-nAChR LSP α4VFL-containing constructs were uniformly monophasic (Fig. 6*A*). This was true whether single or multiple positions were substituted and was independent of which position(s) was altered. Even the three LSP variants where the α4(+)/(−)α4 interface E-loop was not mutated (α4VFL in positions 2, 5, or 2 + 5; see Fig. 1*C*) displayed the same outcome. Even more surprisingly, statistically indistinguishable EC_{50} values (between 7 and 12 μM) were obtained from all of the LSP α4VFL mutant constructs; these EC_{50} values were intermediate between those of the HS (0.6 μM) and LS (≈60 μM) phases of unmutated LSP function (Fig. 6*A* and Table 2). This was true even though there was no change in numbers of α4(+)/(−)β2 or α4(+)/(−)α4 interfaces or even when the α4(+)/(−)α4 interface was replaced by an additional mock α4(+)/(−)β2 interface. In summary, effects of the α4VFL E-loop mutant were completely independent of position and copy number in the LSP α4β2-nAChR isoform. A very similar outcome was observed when introducing α4VFL mutant subunits into the α4β2-nAChR HSP isoform (where none of the mutant subunits could be introduced into an agonist binding pocket; see Fig. 1*C*). In every case, CRCs of α4VFL HSP mutant constructs remained identical to that of the non-mutant HSP control (EC_{50} ≈2 μM; Fig. 6*B* and Table 2).

Although the agonist-pharmacology effects of α4VFL mutant subunit incorporation into LSP α4β2-nAChR were position- and copy number-independent, this was not the case

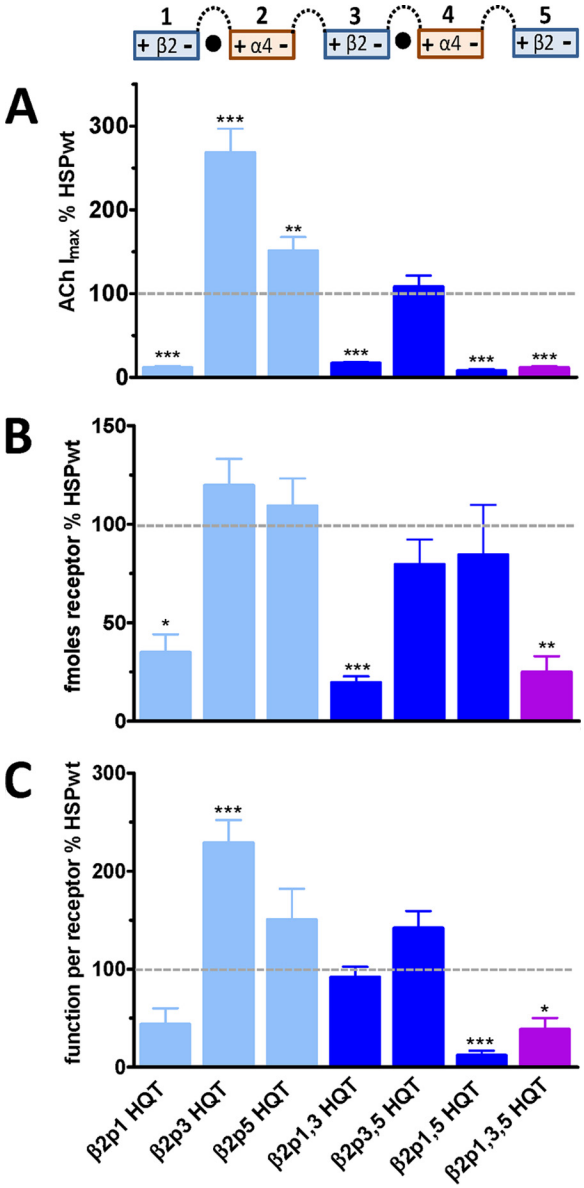

FIGURE 5. **β2HQT E-loop mutation effects on peak ACh-induced function (I_{max}) and nAChR surface expression within HSP concatemers.** Oocytes expressing concatenated HSP constructs incorporating one, two, or three copies of the β2HQT E-loop mutant subunit were screened for maximal ACh current responses, followed by ^{125}I-mAb 295 binding to determine surface nAChR expression (accounting for three β2-binding sites per HSP construct, see "Experimental Procedures"). All results were normalized to the unmutated HSP concatemer for at least three individual experiments (denoted with a *dashed horizontal line* in each panel; see Table 1 for non-normalized data and number of experiments performed). *A*, I_{max} was reduced ~90% for the four HSP constructs harboring β2HQT mutations in position 1, although the single position 3 and 5 variants significantly increased peak current. There was no detectable change for the position 3 + 5 variant. *B*, surface nAChR expression levels were reduced ≈75% in three of the four HSP β2HQT position 1-containing mutants, although the remaining four mutant concatemers had control levels of surface expression. *C*, function per surface nAChR was increased ~2-fold only for the single position 3 HSP mutant, whereas two of the constructs hosting β2HQT in positions 1 + 3 or 1 + 3 + 5 showed significant reductions compared with WT. The remaining four constructs showed no significant changes *versus* control HSP. Because data were collected for the complete set of mutants on the HSP backbone in each individual experiment (see "Experimental Procedures"), including all β2HQT and α4VFL mutant constructs, one-way ANOVA was applied to determine significant differences within the sets of I_{max}, surface expression, or function per receptor values collected on the HSP backbone. One-way ANOVA determined that significant differences existed between groups in each panel: *A*, $F_{11,36} = 65.38$; $p < 0.001$; *B*, $F_{11,33} = 9.1$; $p < 0.001$; *C*, $F_{11,32} = 19.9$; $p < 0.001$. Post hoc comparisons were performed in each case using the Bonferroni correction; differences from the unmutated LSP control are noted as follows: *, $p < 0.05$; **, $p < 0.01$; ***, $p < 0.001$.

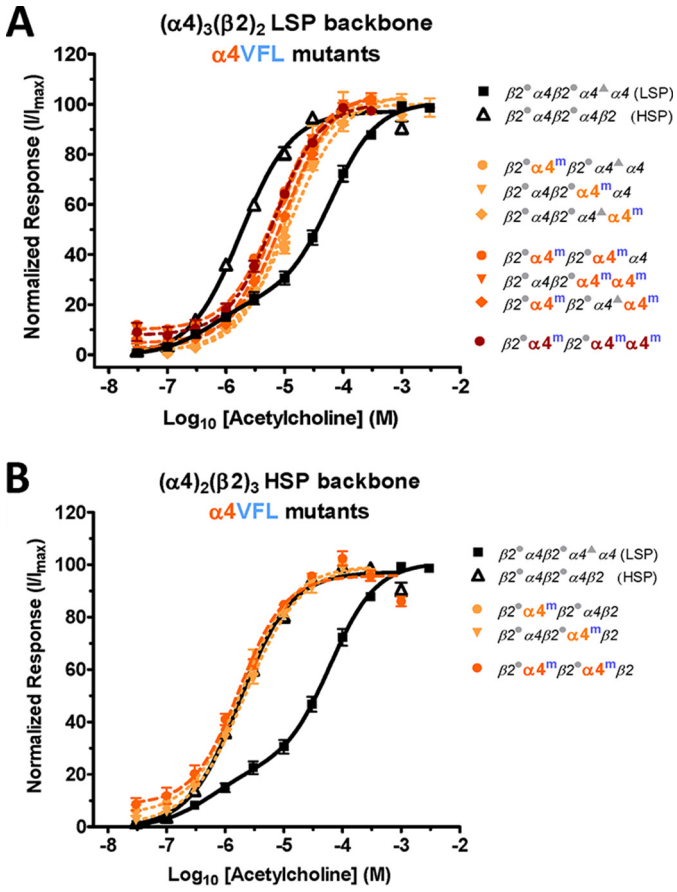

FIGURE 6. **ACh concentration-response profiles for the α4VFL E-loop mutant series of concatenated LS and HS isoforms of α4β2 nAChR.** *A*, oocytes expressing concatenated LSP constructs incorporating one, two, or three copies of the α4VFL E-loop mutant subunit (position(s) indicated by $α4^{m}$) were acutely stimulated with the indicated range of ACh concentrations. CRCs generated from all seven mutant constructs were monophasic with nearly identical EC_{50} values, which were intermediate between the HS and LS phases of the biphasic unmutated LSP construct CRC. *B*, HSP set of three α4VFL E-loop mutant single or double copy concatemers generated CRCs that were indistinguishable from the HSP control. Data points represented the mean (±S.E.) of at least three oocytes and were fit to unconstrained, one-, or two-site logistic equations (most appropriate assignment determined using the extra sum-of-squares *F*-test). Details of the pharmacological parameters calculated and of the applied statistical analyses are reported in Table 2. CRCs obtained from unmodified LSP (■) and HSP (△) parent constructs are included in both graphs for ease of comparison within and between isoforms.

for effects on function per receptor (Fig. 7). As shown in Fig. 7*A*, I_{max} values were significantly reduced for all α4VFL mutant LSP constructs. Qualitatively, the reduction of I_{max} values increased progressively from single- to double- to triple-substituted LSP constructs (Fig. 7*A*). Interestingly, reductions in I_{max} for each of the three single-substituted constructs were largely accounted for by loss of surface expression (Fig. 7*B*); no changes in per nAChR function compared with the unmutated LSP α4β2-nAChR control were measured for any of the single α4VFL-substituted constructs (Fig. 7*C* and Table 2). However, all three of the double α4VFL-substituted LSP constructs produced significantly less per nAChR function compared with the

TABLE 2

Effects of introducing α4VFL E-loop mutant subunits into the LSP and HSP α4β2 nAChR concatemer backgrounds (ACh CRCs)

Oocytes injected with cRNA encoding concatenated LSP or HSP α4β2-nAChR constructs containing zero (LSP or HSP controls), one, or more copies of the α4VFL subunit at the position(s) shown in orange type were used in conjunction with TEVC to establish and analyze ACh CRCs (see Fig. 6, "Experimental Procedures"). Pharmacological parameters were determined as described in the legend to Table 1. Additionally, data representing ACh-activated maximal function (I_{max} in nA, rounded to 1 or 2 significant digits) and I_{max} values corrected for surface nAChR (microampere/fmol) were generated from (*N*) experiments testing six individual oocytes per concatemer per experiment (See Figs. 7 and 8 for these data shown relative to, and compared with, those obtained from control LSP and HSP concatemers respectively). Number of individual oocytes tested is given as *n*.

Concatemer	*ACh (Log_{10} M) EC_{50} (HS)*	*ACh (Log_{10} M) EC_{50} (LS)*	*HS Fraction*	*n*	*ACh I_{max} (nA)*	*μA/fmol*	*N*
β2α4β2α4α4 (LSP)	**-6.25 ± 0.35**	**-4.20 ± 0.10†††**	**0.23 ± 0.12**	**10**	**3900 ± 260**	**194.6 ± 33.8**	**7**
β2α4β2α4α4		-4.91 ± 0.04††	*lost*	3	1300 ± 180	252.7 ± 62.4	6
β2α4β2α4α4		-5.06 ± 0.05†	*lost*	3	2300 ± 260	251.6 ± 133.4	6
β2α4β2α4α4		-5.02 ± 0.03††	*lost*	3	1900 ± 170	269.4 ± 77.6	6
β2α4β2α4α4		-5.15 ± 0.02††	*lost*	4	210 ± 30	96.9 ± 24.2	4
β2α4β2α4α4		-5.15 ± 0.02††	*lost*	4	450 ± 60	104.4 ± 16.3	6
β2α4β2α4α4		-5.00 ± 0.03†††	*lost*	4	220 ± 30	85.8 ± 13.5	7
β2α4β2α4α4		-5.17 ± 0.03†††	*lost*	12	30 ± 4	6.4 ± 0.1	7
β2α4β2α4β2 (HSP)	**-5.75 ± 0.03**			**11**	**500 ± 40**	**19.3 ± 4.7**	**4**
β2α4β2α4β2	-5.72 ± 0.04			5	90 ± 20	10.3 ± 1.2	3
β2α4β2α4β2	-5.66 ± 0.03			6	130 ± 20	10.9 ± 1.4	4
β2α4β2α4β2	-5.76 ± 0.05			9	20 ± 3	5.3 ± 0.6	4

† One-way ANOVA was used to determine differences across log_{10} EC_{50} values obtained from α4VFL-mutant variations on the LSP backbone, as described in Table 1. All α4VFL mutant constructs produced monophasic CRCs, unlike the biphasic CRC of the parent, unmodified, LSP control. *Post hoc* comparisons using the Bonferroni correction demonstrated that the log_{10} EC_{50} values for all LSP-backbone α4VFL-variant CRCs formed a single group, with lower ACh sensitivity than the HS-phase response of the control construct. Differences from the HS-phase response are shown as: †, $p < 0.05$; ††, $p < 0.01$; †††, $p < 0.001$. In contrast, no significant differences were found by ANOVA among log_{10} EC_{50} values derived from the universal monophasic responses of the HSP control construct, and α4VFL mutant variants thereof. All responses were therefore classified as HS-like.

unaltered α4β2-nAChR LSP control. This loss of per nAChR function was primarily driven by an ~50% loss of I_{max}, because changes in surface expression were quite similar across the range of single, double, and triple α4VFL-substituted LSP constructs. As shown in Fig. 7*C* and Table 2, the loss of function/nAChR was the same in all three of the double α4VFL-substituted LSP constructs. The trend was extended in the case of the triple α4VFL-substituted LSP construct, where a further reduction (to ~3% of control) in per receptor function was seen (Fig. 7*C* and Table 2). In conclusion, function/nAChR effects of α4VFL substitution into α4β2-nAChR LSP are position-independent but are copy number-dependent.

This position-independent but copy number-dependent effect of α4VFL substitution was also seen in the α4β2-nAChR HSP background (Fig. 8). α4VFL substitution into either or both available α4 subunit positions suppressed I_{max} significantly compared with control and reduced nAChR surface expression by a little over 50% (Fig. 8, *A* and *B*). When function was normalized to a per nAChR basis, the two single-substituted α4VFL α4β2-nAChR HSP variants exhibited a similar not-quite-significant trend to lower function, although the double-substituted construct produced significantly less function (approximately a 75% reduction; Fig. 8*C* and Table 2) when compared with the unmodified α4β2-nAChR HSP construct.

Mutant E-loop Concatenated and Unlinked α4β2-nAChR Subunit Results Compare Favorably—As shown previously, α4β2-nAChR pentameric and concatemeric constructs can be expressed without degradation and/or rearrangement of subunit ordering (21, 35, 36). Importantly, these previous studies demonstrate that concatenated subunit pentameric constructs

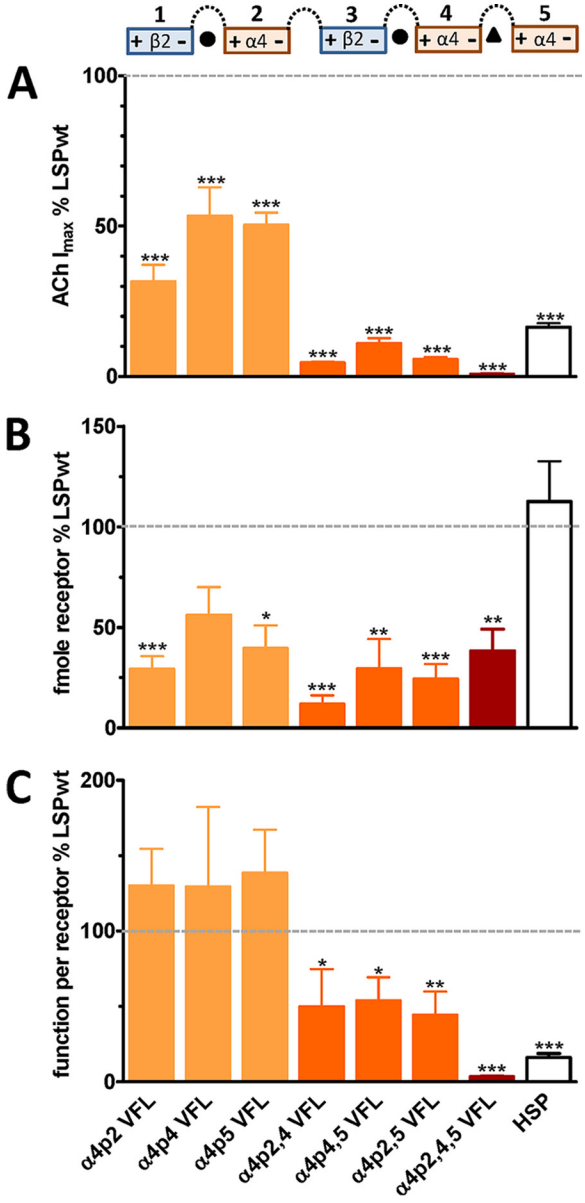

FIGURE 7. **α4VFL E-loop mutation effects on peak ACh-induced function (I_{max}) and nAChR surface expression within LSP concatemers.** Oocytes expressing concatenated LSP constructs incorporating one, two, or three copies of the α4VFL E-loop mutant subunit were screened for maximal ACh current responses, followed by ^{125}I-mAb 295 binding to determine surface nAChR expression. All results were normalized to the unmutated LSP concatemer for at least four individual experiments (denoted with a *dashed horizontal line* in each panel; see Table 2 for the exact number of experiments performed in each case). *A*, I_{max} was reduced in all seven members of the α4VFL mutant series of constructs in a copy-dependent, position-independent manner. Single copies of α4VFL reduced function by ~50%, double copies by ≈90%, and the triple copy variant exhibited a 99% loss of function *versus* the unmodified LSP control. *B*, surface nAChR expression levels were reduced 50–80% in all seven of the LSP α4VFL mutants independent of position or copy number. *C*, function per surface nAChR retained copy dependence and position independence for all mutant constructs as in *A*. α4VFL single copy constructs had WT levels of LSP function; double copies saw a 50% drop in function, and the triple mutant lost 97% of its per receptor function. One-way ANOVA was performed as described in the legend to Fig. 4 and determined that significant differences existed between groups in each panel. Post hoc comparisons were made using the Bonferroni correction; differences from the unmutated LSP control are noted as follows: *, $p < 0.05$; **, $p < 0.01$; ***, $p < 0.001$.

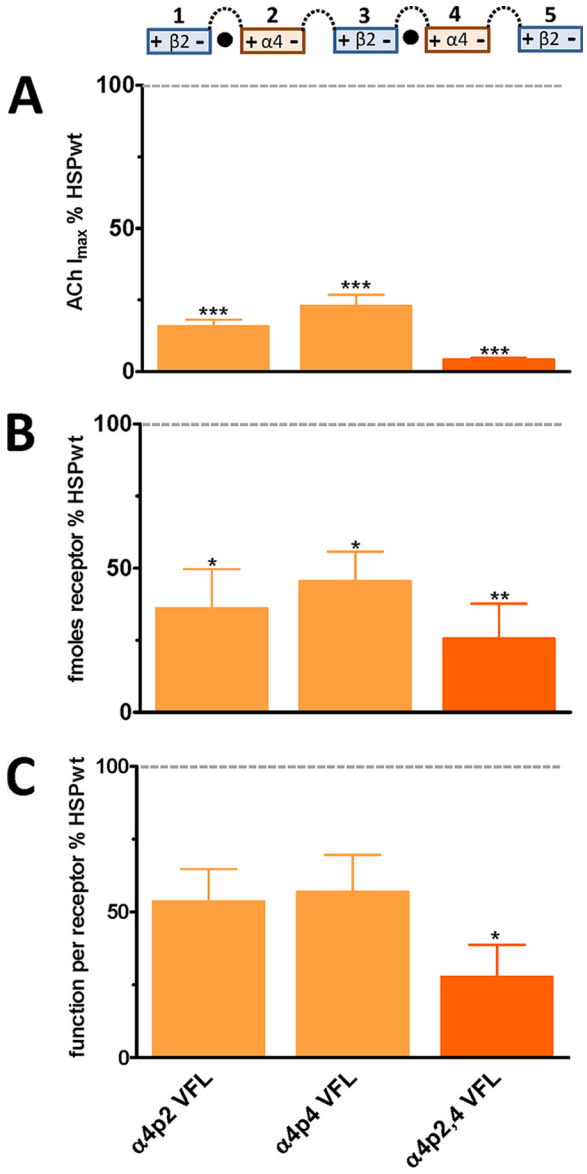

FIGURE 8. **α4VFL E-loop mutation effects on peak ACh-induced function (I_{max}) and nAChR surface expression within HSP concatemers.** Oocytes expressing concatenated HSP constructs incorporating one or two copies of the α4VFL E-loop mutant subunit were screened for maximal ACh current responses, followed by ^{125}I-mAb 295 binding to determine surface nAChR expression. All results were normalized to the unmutated HSP concatemer for at least three individual experiments (denoted with a *dashed horizontal line* in each panel; see Table 2 for the exact number of experiments performed in each case). *A*, I_{max} was reduced in all three of the α4VFL mutant constructs in a copy-dependent, position-independent manner with both single copies reduced ~75%, and the double copy showed a 95% functional loss *versus* the HSP control. *B*, surface nAChR expression levels were reduced 60–75% in all three of the HSP α4VFL mutants. *C*, function per surface nAChR retained copy dependence and position independence for all mutant constructs as in *A*. Both α4VFL single copy constructs had similar reductions of function per receptor but did not quite reach statistical significance *versus* the level of non-mutated HSP function. The double copy variant saw a significant ≈75% drop in function. One-way ANOVA was performed as described in the legend to Fig. 5 and determined that significant differences existed between groups in each panel. Post hoc comparisons were made using the Bonferroni correction; differences from the unmutated LSP control are noted as follows: *, $p < 0.05$; **, $p < 0.01$; ***, $p < 0.001$.

are capable of accurately replicating the salient functional pharmacological features of HS and LS α4β2-nAChR isoforms. To test this point further, we compared results from the concatemeric constructs used in this study to those obtained using unlinked α4 and β2 subunits. This was done using wild-type α4 and β2 subunits, and β2HQT and α4VFL mutant subunits, injected at ratios known to favor formation of HS or LS α4β2-nAChR isoforms. Further comparisons were made to previously published results using these mutant subunits (34). Where subunit compositions were comparable, the results remained extremely similar to each other across our concatemeric (Tables 1 and 2) and our unlinked nAChR subunit experiments (Table 3). Both levels of functional expression and ACh sensitivities match previous findings by others and for receptors of like construction whether from linked or unlinked subunits.

TABLE 3

E-loop mutation effects on ACh-mediated function in unlinked HS and LS α4β2 nAChR isoforms

Oocytes were injected with biased ratios of RNA encoding unlinked wt, α4VFL, or β2HQT subunits to generate predominantly HS $(\alpha4)_2(\beta2)_3$- or LS $(\alpha4)_3(\beta2)_2$-nAChR isoforms (see "Experimental Procedures" for details). ACh-activated I_{max} and CRC $\log_{10}$ (M) EC_{50} values collected in this study are shown in regular font. Previously published (34) injection ratios and pharmacological parameters generated from nAChR containing the indicated wt or E-loop mutant subunits are shown (in parentheses and italicized) for comparison, where possible; ND = not determined. Numbers of oocytes tested are shown for both our, and the previously-published, results.

			ACh ($\log_{10}$ M)				
Subunits	*Isoform bias*	*Injection Ratio*	*Imax (nA)*	*EC_{50} (HS)*	*EC_{50} (LS)*	*HS fraction*	*n*
α4:β2	HS	1:10	470 ± 107	-5.65 ± 0.03			6
		(1:4)	*(920)*	*(-5.80)*			*(6)*
	LS[a]	10:1	2800 ± 260	-5.46 ± 0.52	-3.97 ± 0.1	0.35 ± 0.25	6
		(4:1)	*(3800)*	*(-6.02)*	*(-4.08)*	*(0.16)*	*(17)*
α4VFL:β2	HS	1:10	140 ± 43	-5.72 ± 0.03			8
		(1:4)	*(360)*	*(-6.01)*			*(7)*
	LS	10:1	430 ± 87	-5.43 ± 0.04			3
		(4:1)	*(1400)*	*(-5.49)*			*(8)*
α4:β2HQT	HS	1:10	130 ± 22	-3.79 ±0.02			6
		(1:4)	*(ND)*	*(ND)*			*(ND)*
	LS	10:1	2800 ± 360	-3.64 ± 0.02			6
		(4:1)	*(6600)*	*(-3.85)*			*(7)*
α4VFL:β2HQT	HS[b]	1:10	60 ± 13	-3.85 ± 0.02			7
		(1:4)	*(ND)*	*(ND)*			*(ND)*
	LS[c]	10:1	240 ± 55	-3.91 ± 0.01			8
		(4:1)	*(ND)*	*(ND)*			*(ND)*

[a] Extra sum-of-squares *F*-test indicates a preferred biphasic fit: $F_{5,54} = 11.8$; $p < 0.0001$.
[b] The concatenated version of this all-position-mutated HS isoform had an I_{max} of 6 ± 1 nA ($n = 22$) and an ACh CRC ($\log_{10}$ M) $EC_{50} = -3.98 \pm 0.01$ ($n = 10$).
[c] The concatenated version of this all-position-mutated LS isoform was non-functional.

Mutant E-loop Effects on α4β2-nAChR CRCs Are Similar between ACh and Nicotine—To determine whether the effects of E-loop mutations on ACh potency were unique, or whether they might be more generalizable, we performed an equivalent set of CRC experiments for nicotine (Fig. 9 and Table 4). Although nicotine is less discriminating between HS and LS phase function than ACh (24), very similar outcomes were clearly visible (compare outcomes in Fig. 9 to those in Figs. 2 and 6). Mutant constructs that exhibited increased ACh potency also showed increased nicotine potency. Mutant constructs that exhibited decreased ACh potency also did so for nicotine. Most compellingly, the position-1 β2HQT HSP backbone variant showed a significantly shallower Hill slope for nicotine activation and a significantly decreased $\log_{10}$ EC_{50} value. These are indicators of a composite CRC containing a new nicotine-evoked response component with lower nicotine sensitivity compared with the parent construct (as seen for the same construct when stimulated with the more HS *versus* LS phase-discriminating agonists ACh and A-85380 (Figs. 2 and 3).

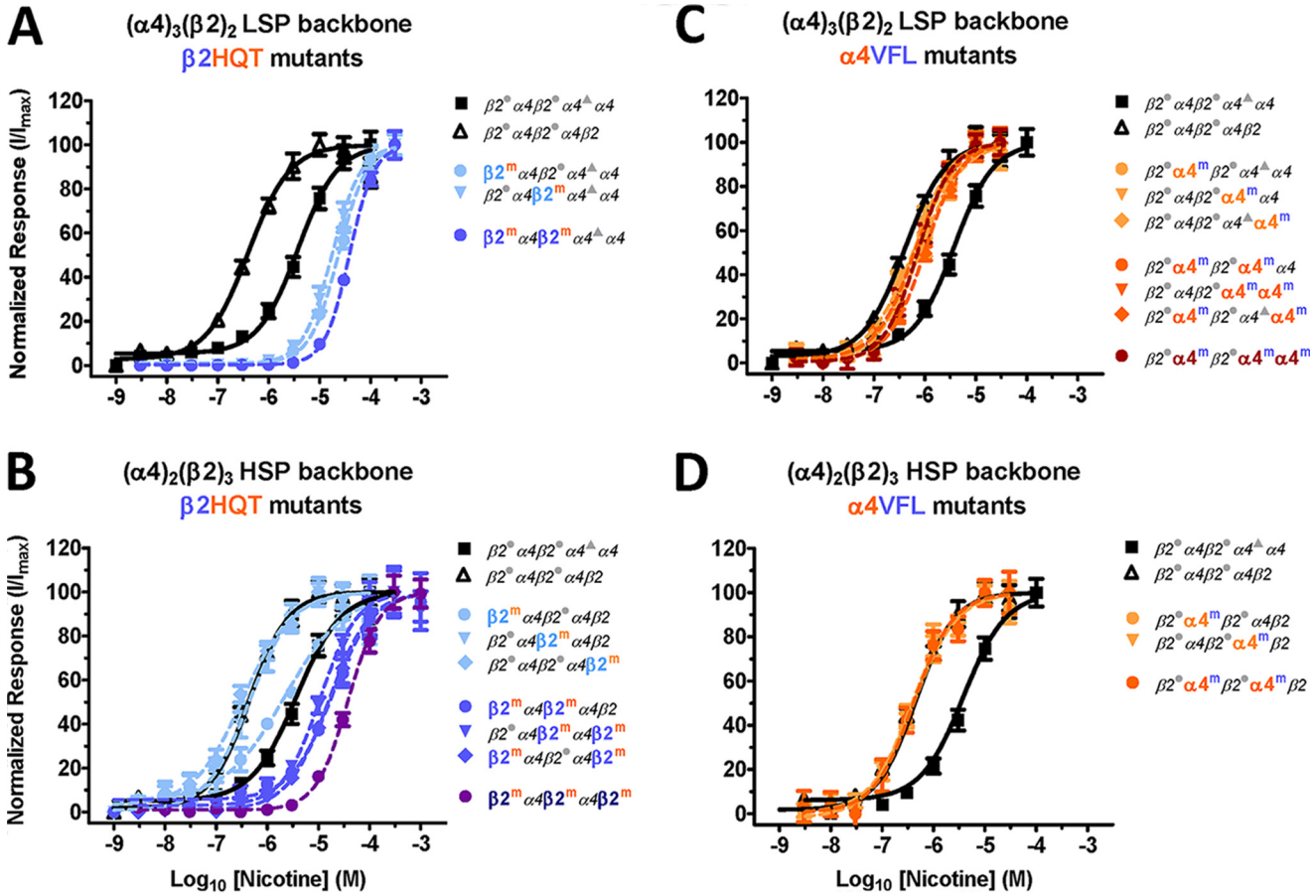

FIGURE 9. **Nicotine concentration-response profiles for the β2HQT and α4VFL E-loop mutant series of concatenated LS and HS α4β2-nAChR isoforms.** Oocytes expressing concatenated LSP (*A*) or HSP (*B*) constructs incorporating one or more copies of the β2HQT E-loop mutant subunit (position(s) indicated by $\beta2^m$) were acutely stimulated with the indicated range of nicotine concentrations. Responses were normalized to the maximum current measured for each individual oocyte. Corresponding CRC data are shown for concatenated LSP (*C*) or HSP (*D*) constructs incorporating one or more copies of the α4VFL E-loop mutant subunit (position(s) indicated by $\alpha4_m$). Details of the obtained pharmacological parameters and the statistical analysis used to compare results are provided in Table 4. Data points represent the mean (±S.E.) of at least six oocytes (numbers provided in Table 4). CRCs obtained using wild-type LSP (■) and HSP (△) parent constructs are included in both graphs for ease of comparison within and between isoforms.

Discussion

Major Findings, Differential Functional Effects of Mutating Nominally Identical α4(+)/(−)β2 Agonist Binding Pockets; Dependence on HSP Versus LSP Background—In a pioneering study, it was first noted explicitly that LS isoform α4β2-nAChR produce a small proportion of intrinsic HS-like function (34). Our subsequent finding was that this fraction of HS phase function produced by the LS isoform was similar in terms of function per receptor to the entire response of HS isoform α4β2-nAChR (36). These data suggested that HS phase function in both α4β2-nAChR isoforms may be produced by activation of the pair of α4(+)/(−)β2 interfaces common to each isoform. This concept was reinforced by two further observations (36). First, HS phase function could be selectively eliminated by predesensitization with the strongly HS activation-preferring compounds sazetidine-A and A-85380. Second, mutations at the α4(+)/(−)α4 site of LS isoform α4β2-nAChR preferentially reduced LS phase function. However, both these studies, and a further one reinforcing the importance of α4(+)/(−)α4 site engagement for effective activation of LS isoform α4β2-nAChR (37) implicitly treated the two α4(+)/(−)β2 agonist-binding sites as an equivalent pair.

As outlined in the Introduction, our hypothesis stated that the two canonical agonist-binding sites might contribute differentially to activation (both within each isoform and between the two isoforms). This possibility arises because the environments in which the agonist sites are found are not identical; subunits that contribute the α4(+)/(−)β2 agonist-binding sites are surrounded by different neighbors. Please note that because our experiments with ACh and nicotine both produced very similar outcomes, we will henceforth predominantly discuss only our data obtained with ACh, for the sake of clarity. An overview of our major findings is presented in Fig. 10. It illustrates that insertion of the E-loop β2HQT mutant at one or the other of the two apparently equivalent α4(+)/(−)β2 agonist-binding sites in the HS α4β2-nAChR isoform produces different changes in ACh sensitivity and/or levels of function per surface nAChR. We also demonstrate that nominally identical changes made at the same α4(+)/(−)β2 interfaces in the LS α4β2-nAChR isoform give markedly different functional outcomes from those seen on the HS isoform background. We conclude that the two conserved α4(+)/(−)β2 agonist-binding sites contribute differently to HS α4β2-nAChR isoform function and between LS and HS α4β2-nAChR isoforms.

TABLE 4

Effects of introducing β2HQT or α4VFL E-loop mutant subunits into the LSP and HSP α4β2 nAChR concatemer backgrounds (nicotine CRCs)

Oocytes injected with RNA encoding concatenated LSP or HSP α4β2-nAChR constructs containing zero (LSP or HSP controls), one, or more copies of the β2HQT or α4VFL subunits at the position(s) shown in blue or orange type, respectively, were used in conjunction with two-electrode voltage clamp to establish and analyze nicotine CRCs (see Fig. 9, "Experimental Procedures"). Pharmacological parameters were determined as previously described for ACh, and are presented as means ± S.E. Numbers of oocytes tested for each parent construct or variant are indicated, and data were collected across three biological replicates. Because nicotine is less discriminating than ACh, none of the CRCs could be fit using a two-site model (fits would not converge). Accordingly, single-site fits were applied to data from all constructs. The resulting Hill slope values were uniformly close to 1, with the exception of HSP β2HQT position 1 (0.73 ± 0.09 *versus.* 1.06 ± 0.10 for unmodified HSP; $p = 0.037$ by Student's t test).

Concatemer (β2HQT variants)	*Nicotine* log_{10} EC_{50} *(M)*	*n*	*Concatemer* (α4VFL variants)	*Nicotine* log_{10} EC_{50} *(M)*	*n*
β2α4β2α4α4 (LSP)	**-5.43 ± 0.06**	**9**	**β2α4β2α4α4 (HSP)**	**-6.35 ± 0.11**	**8**
β2α4β2α4α4	-4.63 ± 0.04****	6	β2α4β2α4β2	-6.39 ± 0.08	7
β2α4β2α4α4	-4.76 ± 0.04****	10	β2α4β2α4β2	-6.43 ± 0.08	6
β2α4β2α4α4	-4.41 ± 0.03****	6	β2α4β2α4β2	-6.38 ± 0.10	7
β2α4β2α4β2 (HSP)	**-6.35 ± 0.11**	**8**	**β2α4β2α4α4 (LSP)**	**-5.43 ± 0.06**	**9**
β2α4β2α4β2	-5.66 ± 0.08****	6	β2α4β2α4α4	-6.10 ± 0.07****	6
β2α4β2α4β2	-6.35 ± 0.08	7	β2α4β2α4α4	-6.23 ± 0.08****	6
β2α4β2α4β2	-6.48 ± 0.07	6	β2α4β2α4α4	-6.21 ± 0.05****	8
β2α4β2α4β2	-4.73 ± 0.07****	9	β2α4β2α4α4	-6.19 ± 0.06****	6
β2α4β2α4β2	-4.97 ± 0.06****	6	β2α4β2α4α4	-6.14 ± 0.05****	7
β2α4β2α4β2	-4.80 ± 0.07****	6	β2α4β2α4α4	-6.00 ± 0.05****	7
β2α4β2α4β2	-4.42 ± 0.04****	9	β2α4β2α4α4	-6.14 ± 0.06****	6

**** One-way ANOVA was used to determine differences across log_{10} EC_{50} values obtained from β2HQT and α4VFL mutant variations on the HSP and LSP backbones ($F_{11,74} = 113.2$, $p < 0.0001$, and $F_{11,73} = 127.5$, $p < 0.0001$, respectively). Post hoc comparisons using the Bonferroni correction were used to identify variant constructs with significantly different log_{10} EC_{50} values compared to those calculated for their parent HSP or LSP backbone constructs.

Introduction of β2HQT subunits has been proved to alter agonist binding at α4(+)/(−)β2 interfaces, making it resemble more closely binding at an α4(+)/(−)α4 site (34, 38). In this study, placement of β2HQT mutant subunits into the (−)-side of the conserved canonical α4(+)/(−)β2 agonist binding interfaces produced very similar outcomes in the LSP $(\alpha4)_3(\beta2)_2$ isoform. For example, β2HQT insertion into either possible position produced indistinguishable changes in agonist pharmacology and per receptor function. These outcomes indicate that, in partial contradiction of our original hypothesis, the two canonical α4(+)/(−)β2 agonist-binding sites within the LS isoform α4β2-nAChR likely contribute in similar ways to receptor activation.

However, the same is not true in the context of the HS isoform. Here, β2HQT insertion into the first *versus* the second concatemeric α4(+)/(−)β2 agonist binding interface resulted in dramatically different ACh CRC outcomes. Effects on per receptor function also differed considerably between these two singly substituted HSP mutants. These results are the first demonstration that, despite the fact that the composition of these canonical α4(+)/(−)β2 agonist-binding sites is completely conserved, they make significantly different contributions to HS isoform α4β2-nAChR activation. This finding is in marked contrast to the position-independent situation in LS isoform α4β2-nAChR (Fig. 10). Together, these two outcomes confirm our original hypothesis.

Effects of α4VFL Mutant Subunit Introduction, Position and Background Independence—The HSP-α4β2-nAChR construct contains no α4(+)/(−)α4 interfaces, so no direct effect would be anticipated on agonist binding following introduction of the E-loop α4VFL mutation into α4(−)-interfaces. As shown in Fig. 6*B*, this expectation was met; CRCs were indistinguishable across all of the α4β2-HSP constructs. Effects on surface expression and per receptor function were noted, and these were symmetrical (Figs. 7, *B* and C, and 10). Similar trends were observed for per receptor function.

However, results from the LSP-α4β2-nAChR construct family, all members of which *do* contain an α4(+)/(−)α4 interface, were much more surprising. Here, substitution of the α4VFL mutant subunit into any position, or combination of positions, resulted in an identical outcome (Fig. 6*A*). Similar to the outcome seen in the α4β2-HSP-nAChR context, LSP per receptor function was progressively reduced as the number of α4VFL mutant subunits introduced was increased, and no position dependence was seen (Figs. 7*C* and 10). These findings are surprising given that the α4(+)/(−)α4 interface within the α4β2-LS-nAChR isoform has been shown directly, by multiple approaches, to correspond to an agonist-binding site (35, 36). From these findings, we conclude that α4(−)-face E-loop contributions to α4β2-nAChR function are principally allosteric at both isoforms (rather than being dominated by direct interactions with ACh at the α4(+)/(−)α4-binding site, in the context of the LS isoform). This is not to imply that other parts of the α4(+)/(−)α4-binding site do not directly interact with ACh or other agonists; in fact our work and the work of others indicates that they do (35–37).

Value of Using Tethered nAChR Pentamers and nAChR Cell Surface Binding Assays—The concatenated nAChR subunit approach offers substantial advantages in terms of expressing completely defined nAChR subtypes, including difficult-to-combine subunits (39, 40, 44). It also allows site-directed mutagenesis to be targeted to particular subunits when multiple copies are present in a pentameric complex (35–37). As shown in Tables 1–3, functional parameters are very similar across all comparable nAChR compositions, whether expressed from linked or unlinked subunits. Critically, this validates the utility of concatemeric nAChR as a model in our studies of position-by-position subunit manipulation and our central discoveries revealed by systematic nAChR subunit interface alterations.

This study also illustrates the importance of measuring the effects of subunit mutation on cell surface expression of pure nAChR populations. Without the ability to normalize for cell surface nAChR expression, interpretation of differences between constructs in ion channel function *per se* would not be possible.

Although it is certainly true that precise interpretation of structure-activity relationships using only macroscopic CRCs can be problematic (48), previously published results allow us to make predictions. Changes in function per receptor must arise from altered single-channel conductance and/or open probability. A previous study of HS and LS isoform single-channel amplitudes indicates that the LS isoform may be associated with higher calculated chord conductance than the HS isoform (29 *versus* 21 picosiemens, respectively (22)). However, this difference is far less than required to account for the difference in function per receptor for these two isoforms as measured in this

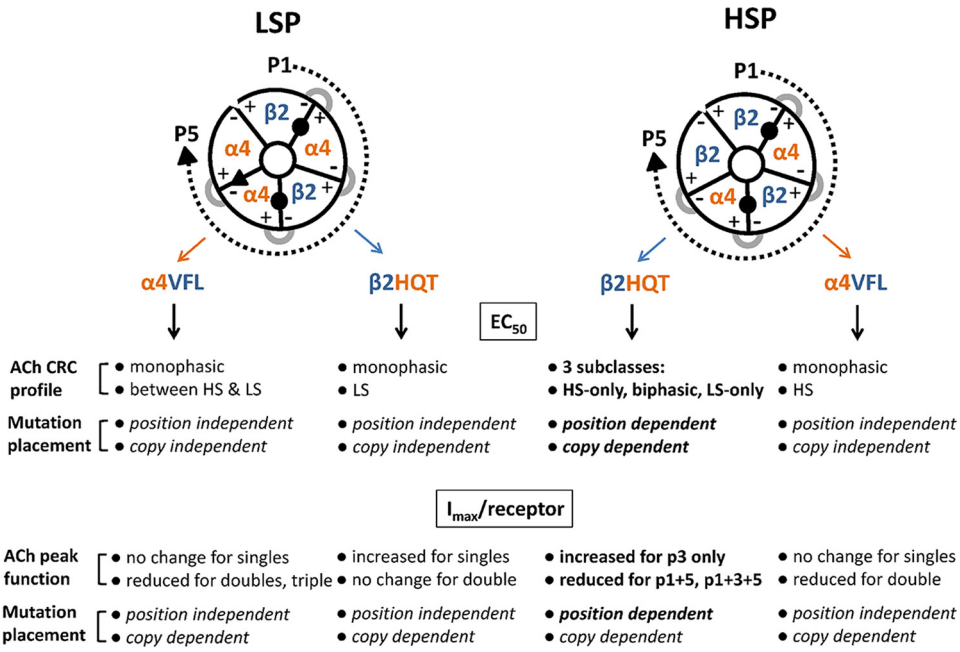

FIGURE 10. **Reciprocal E-loop mutations placed within or outside of α4(+)/(−)β2 nAChR agonist binding interfaces reveal intra- and inter-isoform functional differences.** An overview is provided of the major findings generated by employing systematic E-loop substitution in concatenated α4β2-nAChR isoforms. In the case of the β2HQT series of concatemers (*center columns*), E-loop probing revealed differential functional effects of altering nominally identical α4(+)/(−)β2-binding sites within the HSP background (outcomes were strongly dependent on position and copy number for EC_{50} and I_{max}/nAChR determinations). Contrasting results were seen following ostensibly identical manipulations performed on the LSP background (outcomes were predominantly position-independent). Conversely, α4VFL subunits placed within either isoform (*flanking columns*) yielded highly similar results in terms of within and between the HSP and LSP backgrounds. Position and copy independence was observed when considering EC_{50} values, and position independence and copy dependence were typical features when considering per receptor function. Because functional changes resulting from introduction of the α4VFL mutant subunit were α4(+)/(−)α4 interface-independent, they are likely to be predominantly allosteric in nature, rather than driven by a direct E-loop interaction with agonist at this site.

study (~10-fold greater for LS *versus* HS isoform α4β2-nAChR). Accordingly, we predict that the predominant effect of engaging the α4(+)/(−)α4 allosteric-like site is to increase channel-open probability. This would certainly be compatible with other prior findings. For example, it has been demonstrated that binding to the α4(+)/(−)α4 site is required for full agonist efficacy at LS isoform α4β2-nAChR (37). Furthermore, different parts of the same interface are known to form an allosteric Zn^{2+} potentiation site (49), and it has been shown that the principal effect of Zn^{2+} potentiation on α4β4-nAChR is to increase burst duration and therefore open probability (50). Therefore, it seems reasonable to hypothesize that altered open probabilities will also be the predominant factor driving the often large changes in per receptor function that are induced by incorporation of E-loop mutant subunits. This is especially so because E-loop mutations are located far from the channel domain; direct effects on channel conductance would not be anticipated.

General Rules, Broad Contributions of Particular Subunit Interfaces to α4β2-nAChR Function—Some generalizable features are revealed by viewing our findings first in terms of alterations in agonist-recognizing subunit interfaces. Nearly every time that an α4(+)/(−)β2 interface is converted to a mock α4(+)/(−)α4 interface, the result is an nAChR with LS-like features (EC_{50} value ≥60 μM). Conversely, there is never an LS profile for sensitivity to ACh when a natural α4(+)/(−)α4 interface is eliminated in the LSP backbone. These observations confirm and extend previous findings indicating that introduction of β2HQT subunits at α4(+)/(−)β2 interfaces makes them more closely resemble α4(+)/(−)α4 sites with lower ACh sensitivity (34, 38) and that α4(+)/(−)β2 interfaces contribute to higher agonist sensitivity. However, this approach is not sufficient to explain all of the findings of this study. As already discussed, introduction of an α4VFL mutant subunit *anywhere* in the LS isoform background (not just in the α4(+)/(−)α4 interface) produces a reduction in ACh EC_{50}. In addition, as will be discussed next, this agonist-binding-site-only model is not adequate to explain several more observations.

Exceptions to the General Rules, the Importance of Neighbors and the E-loop—Defining the precisely detailed mechanisms underlying differential α4(+)/(−)β2 agonist site contributions to HS and LS isoform α4β2-nAChR activation (such as changes in binding site affinity, interactions between the multiple binding sites present, and the extent of site-to-site cooperativity) is likely to require a sophisticated and extensive single-channel kinetics analysis, far beyond the scope of this study (48). However, the hypothesis that introducing mutations into the E-loops of α4β2-nAChR isoforms can significantly alter the allosteric activation mechanism of the host nAChR could also apply to β2HQT mutant subunits. In fact, this new hypothesis can explain our further otherwise-surprising observations (in addition to the position independence of the α4VFL subunit's effects).

In the first example, only the position 1 β2HQT mutant on an HSP backbone exhibits biphasic ACh activation (Figs. 2*B* and 3). This concatemer and the LSP construct are the only

ones featuring an α4(+)/(−)α4-like agonist binding pocket flanked by *unmutated* β2 subunits (see *inset* to Fig. 3 for a circularized representation of the assembled position 1 β2HQT HSP construct). In the second example, a single β2HQT mutant-subunit substitution in either position 3 (where it does participate in an α4(+)/(−)β2 agonist binding pocket) or position 5 (where it does not participate in an agonist-binding site) has no effect on the resulting agonist CRCs (Fig. 2*B*). However, combining these two mutations, which are individually without effect, results in a substantial loss of agonist potency. This constitutes direct evidence that the E-loop status of a neighboring subunit can affect the functional contribution of a canonical α4(+)/(−)β2 agonist-binding site. It therefore appears that the functional effects of the β2HQT mutation are mediated allosterically in addition to its recently demonstrated effect on agonist binding potency (38). In the third example, and related to the preceding point, function per nAChR in the HSP β2HQT mutant series (Fig. 5) is significantly reduced only if both subunits at the β2(+)/(−)β2 interface are mutated (HSP β2HQTp1p5, and β2HQTp1p3p5). In addition, on the HSP backbone, the presence of just one α4(+)/(−)β2 interface is adequate to yield HS function except in the presence of β2HQTp5 altering the β2(+)/(−)β2 interface. These observations suggest that a wild-type β2(+)/(−)β2 interface is an important factor in HSP function. As a corollary to this observation, the LSP isoform, which lacks a β2(+)/(−)β2 interface, loses all HS component function with just one β2HQT substitution. Our results imply that E-loop allosteric effects constitute an important part of the context that results in otherwise identical α4(+)/(−)β2 agonist-binding sites contributing differentially to nAChR agonist activation both within HS isoform α4β2-nAChR and between the two α4β2-nAChR isoforms.

Interestingly, the current findings dovetail with and also help to explain observations in other studies (of α6β2*-nAChR) that pointed to the importance of α6 (−)-face E-loop effects on functional levels and agonist sensitivities (51–53). In those publications, mouse (Asp-143 and Val-145) or human (Asn-143 and Met-145) α6 subunit residues determined in a species-specific manner functional effects of β3 subunit co-assembly into α6*-nAChR containing β2 or β4 subunits. These residues are nested between the α4 and β2 subunit E-loop residues that were targeted in this study. A very recent publication (54) also demonstrated interactions of an α4 (−)-face E-loop engineered into the binding pocket of *Lymnaea stagnalis* acetylcholine-binding protein with a neighboring subunit. These interactions differed according to which particular ligand was bound (at least for compounds that are exceptionally selective between HS and LS phase activation), and appeared likely to impact receptor activation (54). If somewhat analogous interactions occur at interfaces not bound by agonist, this may provide at least a partial mechanistic basis for E-loop involvement in the neighbor effects noted in this study.

Our findings illustrate previously unappreciated complexity in the agonist activation mechanism of α4β2-nAChR, which are a predominant and physiologically important non-muscle nAChR subtype. It seems likely that similar phenomena may be seen in other Cys-loop receptors, given the high degree of structural similarity across members of the superfamily.

Author Contributions—L. M. L. assisted with experimental design and interpretation, engineered the new concatenated nAChR constructs used in this study, performed electrophysiology experiments, and assisted with manuscript preparation (including figures and tables). M. M. W. and J. B. E. performed electrophysiology experiments and assisted with manuscript preparation (including figures and tables). J. F. C. produced ^{125}I-mAb 295 and provided essential guidance on experimental design. J. M. L. assisted with manuscript drafting and provided critical revision of its content. R. J. L. assisted with experimental design and interpretation and with manuscript writing and revisions. P. W. conceived and coordinated the study, performed the ^{125}I-mAb 295 binding experiments, and (with advice and counsel from the other authors) was principally responsible for data interpretation and manuscript writing. All authors reviewed the results and approved the final version of the manuscript.

Acknowledgments—We thank Dr. Isabel Bermudez (Oxford Brookes University, Oxford, UK) for providing the original HSP and LSP α4β2 constructs that were modified for use in this study and for extensive advice on their use. We also thank Drs. F. Ivy Carroll (Research Triangle Institute, Research Triangle Park, NC) and Alan P. Kozikowski (University of Illinois, Chicago) for gifts of compounds.

References

1. Gotti, C., Clementi, F., Fornari, A., Gaimarri, A., Guiducci, S., Manfredi, I., Moretti, M., Pedrazzi, P., Pucci, L., and Zoli, M. (2009) Structural and functional diversity of native brain neuronal nicotinic receptors. *Biochem. Pharmacol.* **78,** 703–711
2. Marks, M. J., Laverty, D. S., Whiteaker, P., Salminen, O., Grady, S. R., McIntosh, J. M., and Collins, A. C. (2010) John Daly's compound, epibatidine, facilitates identification of nicotinic receptor subtypes. *J. Mol. Neurosci.* **40,** 96–104
3. Lindstrom, J. M. (2003) Nicotinic acetylcholine receptors of muscles and nerves: comparison of their structures, functional roles, and vulnerability to pathology. *Ann. N. Y. Acad. Sci.* **998,** 41–52
4. Cordero-Erausquin, M., Marubio, L. M., Klink, R., and Changeux, J. P. (2000) Nicotinic receptor function: new perspectives from knockout mice. *Trends Pharmacol. Sci.* **21,** 211–217
5. Steinlein, O. K. (2001) Genes and mutations in idiopathic epilepsy. *Am. J. Med. Genet. B.* **106,** 139–145
6. Picciotto, M. R., Zoli, M., Léna, C., Bessis, A., Lallemand, Y., Le Novère, N., Vincent, P., Pich, E. M., Brûlet, P., and Changeux, J. P. (1995) Abnormal avoidance-learning in mice lacking functional high-affinity nicotine receptor in the brain. *Nature* **374,** 65–67
7. Govind, A. P., Vezina, P., and Green, W. N. (2009) Nicotine-induced upregulation of nicotinic receptors: underlying mechanisms and relevance to nicotine addiction. *Biochem. Pharmacol.* **78,** 756–765
8. Dani, J. A., and Bertrand, D. (2007) Nicotinic acetylcholine receptors and nicotinic cholinergic mechanisms of the central nervous system. *Annu. Rev. Pharmacol. Toxicol.* **47,** 699–729
9. Stitzel, J. A. (2008) Naturally occurring genetic variability in the nicotinic acetylcholine receptor α4 and α7 subunit genes and phenotypic diversity in humans and mice. *Front. Biosci.* **13,** 477–491
10. Levin, E. D., McClernon, F. J., and Rezvani, A. H. (2006) Nicotinic effects on cognitive function: behavioral characterization, pharmacological specification, and anatomic localization. *Psychopharmacology* **184,** 523–539
11. Hurst, R., Rollema, H., and Bertrand, D. (2013) Nicotinic acetylcholine receptors: from basic science to therapeutics. *Pharmacol. Ther.* **137,** 22–54
12. Coe, J. W., Brooks, P. R., Vetelino, M. G., Wirtz, M. C., Arnold, E. P., Huang, J., Sands, S. B., Davis, T. I., Lebel, L. A., Fox, C. B., Shrikhande, A.,

Heym, J. H., Schaeffer, E., Rollema, H., Lu, Y., *et al.* (2005) Varenicline: an α4β2 nicotinic receptor partial agonist for smoking cessation. *J. Med. Chem.* **48,** 3474–3477
13. Rollema, H., Coe, J. W., Chambers, L. K., Hurst, R. S., Stahl, S. M., and Williams, K. E. (2007) Rationale, pharmacology and clinical efficacy of partial agonists of α4β2 nACh receptors for smoking cessation. *Trends Pharmacol. Sci.* **28,** 316–325
14. Hutchison, K. E., Allen, D. L., Filbey, F. M., Jepson, C., Lerman, C., Benowitz, N. L., Stitzel, J., Bryan, A., McGeary, J., and Haughey, H. M. (2007) CHRNA4 and tobacco dependence–from gene regulation to treatment outcome. *Arch. Gen. Psychiatry* **64,** 1078–1086
15. Voineskos, S., De Luca, V., Mensah, A., Vincent, J. B., Potapova, N., and Kennedy, J. L. (2007) Association of α4β2 nicotinic receptor and heavy smoking in schizophrenia. *J. Psychiatry Neurosci.* **32,** 412–416
16. Saccone, N. L., Schwantes-An, T. H., Wang, J. C., Grucza, R. A., Breslau, N., Hatsukami, D., Johnson, E. O., Rice, J. P., Goate, A. M., and Bierut, L. J. (2010) Multiple cholinergic nicotinic receptor genes affect nicotine dependence risk in African and European Americans. *Genes Brain Behav.* **9,** 741–750
17. Son, C. D., Moss, F. J., Cohen, B. N., and Lester, H. A. (2009) Nicotine normalizes intracellular subunit stoichiometry of nicotinic receptors carrying mutations linked to autosomal dominant nocturnal frontal lobe epilepsy. *Mol. Pharmacol.* **75,** 1137–1148
18. Anand, R., Conroy, W. G., Schoepfer, R., Whiting, P., and Lindstrom, J. (1991) Neuronal nicotinic acetylcholine-receptors expressed in *Xenopus* oocytes have a pentameric quaternary structure. *J. Biol. Chem.* **266,** 11192–11198
19. Cooper, E., Couturier, S., and Ballivet, M. (1991) Pentameric structure and subunit stoichiometry of a neuronal nicotinic acetylcholine receptor. *Nature* **350,** 235–238
20. Zhou, Y., Nelson, M. E., Kuryatov, A., Choi, C., Cooper, J., and Lindstrom, J. (2003) Human α4β2 acetylcholine receptors formed from linked subunits. *J. Neurosci.* **23,** 9004–9015
21. Carbone, A. L., Moroni, M., Groot-Kormelink, P. J., and Bermudez, I. (2009) Pentameric concatenated (α4)(2)(β2)(3) and (α4)(3)(β2)(2) nicotinic acetylcholine receptors: subunit arrangement determines functional expression. *Br. J. Pharmacol.* **156,** 970–981
22. Nelson, M. E., Kuryatov, A., Choi, C. H., Zhou, Y., and Lindstrom, J. (2003) Alternate stoichiometries of α4β2 nicotinic acetylcholine receptors. *Mol. Pharmacol.* **63,** 332–341
23. Zwart, R., and Vijverberg, H. P. (1998) Four pharmacologically distinct subtypes of α4β2 nicotinic acetylcholine receptor expressed in *Xenopus laevis* oocytes. *Mol. Pharmacol.* **54,** 1124–1131
24. Marks, M. J., Whiteaker, P., Calcaterra, J., Stitzel, J. A., Bullock, A. E., Grady, S. R., Picciotto, M. R., Changeux, J. P., and Collins, A. C. (1999) Two pharmacologically distinct components of nicotinic receptor-mediated rubidium efflux in mouse brain require the β2 subunit. *J. Pharmacol. Exp. Ther.* **289,** 1090–1103
25. Gotti, C., Moretti, M., Meinerz, N. M., Clementi, F., Gaimarri, A., Collins, A. C., and Marks, M. J. (2008) Partial deletion of the nicotinic cholinergic receptor α4 or β2 subunit genes changes the acetylcholine sensitivity of receptor-mediated $^{86}Rb^{+}$ efflux in cortex and thalamus and alters relative expression of α4 and β2 subunits. *Mol. Pharmacol.* **73,** 1796–1807
26. Weltzin, M. M., Lindstrom, J. M., Lukas, R. J., and Whiteaker, P. (2015) Distinctive effects of nicotinic receptor intracellular-loop mutations associated with nocturnal frontal lobe epilepsy. *Neuropharmacology* **102,** 158–173
27. Grupe, M., Paolone, G., Jensen, A. A., Sandager-Nielsen, K., Sarter, M., and Grunnet, M. (2013) Selective potentiation of (α4)3(β2)2 nicotinic acetylcholine receptors augments amplitudes of prefrontal acetylcholine- and nicotine-evoked glutamatergic transients in rats. *Biochem. Pharmacol.* **86,** 1487–1496
28. Grupe, M., Grunnet, M., Bastlund, J. F., and Jensen, A. A. (2015) Targeting α4β2 nicotinic acetylcholine receptors in central nervous system disorders: perspectives on positive allosteric modulation as a therapeutic approach. *Basic Clin. Pharmacol. Toxicol.* **116,** 187–200
29. Timmermann, D. B., Sandager-Nielsen, K., Dyhring, T., Smith, M., Jacobsen, A. M., Nielsen, E. Ø., Grunnet, M., Christensen, J. K., Peters, D., Kohlhaas, K., Olsen, G. M., and Ahring, P. K. (2012) Augmentation of cognitive function by NS9283, a stoichiometry-dependent positive allosteric modulator of α2- and α4-containing nicotinic acetylcholine receptors. *Br. J. Pharmacol.* **167,** 164–182
30. Celie, P. H., van Rossum-Fikkert, S. E., van Dijk, W. J., Brejc, K., Smit, A. B., and Sixma, T. K. (2004) Nicotine and carbamylcholine binding to nicotinic acetylcholine receptors as studied in AChBP crystal structures. *Neuron* **41,** 907–914
31. Brejc, K., van Dijk, W. J., Smit, A. B., and Sixma, T. K. (2002) in *Ion Channels: From Atomic Resolution Physiology to Functional Genomics* (Bock, G. and Goode, J. A., eds) pp. 22–32, John Wiley and Sons, Ltd., Chichester, UK
32. Corringer, P. J., Le Novère, N., and Changeux, J. P. (2000) Nicotinic receptors at the amino acid level. *Annu. Rev. Pharmacol. Toxicol.* **40,** 431–458
33. Xiu, X., Puskar, N. L., Shanata, J. A., Lester, H. A., and Dougherty, D. A. (2009) Nicotine binding to brain receptors requires a strong cation-π interaction. *Nature* **458,** 534–537
34. Harpsøe, K., Ahring, P. K., Christensen, J. K., Jensen, M. L., Peters, D., and Balle, T. (2011) Unraveling the high- and low-sensitivity agonist responses of nicotinic acetylcholine receptors. *J. Neurosci.* **31,** 10759–10766
35. Mazzaferro, S., Benallegue, N., Carbone, A., Gasparri, F., Vijayan, R., Biggin, P. C., Moroni, M., and Bermudez, I. (2011) Additional acetylcholine (ACh) binding site at α4/α4 interface of $(\alpha4\beta2)_2\alpha4$ nicotinic receptor influences agonist sensitivity. *J. Biol. Chem.* **286,** 31043–31054
36. Eaton, J. B., Lucero, L. M., Stratton, H., Chang, Y., Cooper, J. F., Lindstrom, J. M., Lukas, R. J., and Whiteaker, P. (2014) The unique α4(+)/(−)α4 agonist-binding site in $(\alpha4)_3(\beta2)_2$ subtype nicotinic acetylcholine receptors permits differential agonist desensitization pharmacology versus the $(\alpha4)_2(\beta2)_3$ subtype. *J. Pharmacol. Exp. Ther.* **348,** 46–58
37. Mazzaferro, S., Gasparri, F., New, K., Alcaino, C., Faundez, M., Iturriaga Vasquez, P., Vijayan, R., Biggin, P. C., and Bermudez, I. (2014) Non-equivalent ligand selectivity of agonist sites in (α4β2)2α4 nicotinic acetylcholine receptors: a key determinant of agonist efficacy. *J. Biol. Chem.* **289,** 21795–21806
38. Ahring, P. K., Olsen, J. A., Nielsen, E. Ø., Peters, D., Pedersen, M. H., Rohde, L. A., Kastrup, J. S., Shahsavar, A., Indurthi, D. C., Chebib, M., Gajhede, M., and Balle, T. (2015) Engineered α4β2 nicotinic acetylcholine receptors as models for measuring agonist binding and effect at the orthosteric low-affinity α4–α4 interface. *Neuropharmacology* **92,** 135–145
39. George, A. A., Lucero, L. M., Damaj, M. I., Lukas, R. J., Chen, X., and Whiteaker, P. (2012) Function of human α3β4α5 nicotinic acetylcholine receptors is reduced by the α5(D398N) variant. *J. Biol. Chem.* **287,** 25151–25162
40. Moretti, M., Zoli, M., George, A. A., Lukas, R. J., Pistillo, F., Maskos, U., Whiteaker, P., and Gotti, C. (2014) The novel α7β2-nicotinic acetylcholine receptor subtype is expressed in mouse and human basal forebrain: biochemical and pharmacological characterization. *Mol. Pharmacol.* **86,** 306–317
41. Whiting, P., and Lindstrom, J. (1987) Purification and characterization of a nicotinic acetylcholine-receptor from rat-brain. *Proc. Natl. Acad. Sci. U.S.A.* **84,** 595–599
42. Lai, A., Parameswaran, N., Khwaja, M., Whiteaker, P., Lindstrom, J. M., Fan, H., McIntosh, J. M., Grady, S. R., and Quik, M. (2005) Long-term nicotine treatment decreases striatal α6 nicotinic acetylcholine receptor sites and function in mice. *Mol. Pharmacol.* **67,** 1639–1647
43. Whiteaker, P., Cooper, J. F., Salminen, O., Marks, M. J., McClure-Begley, T. D., Brown, R. W., Collins, A. C., and Lindstrom, J. M. (2006) Immunolabeling demonstrates the interdependence of mouse brain α4 and β2 nicotinic acetylcholine receptor subunit expression. *J. Comp. Neurol.* **499,** 1016–1038
44. Kuryatov, A., and Lindstrom, J. (2011) Expression of functional human α6β2β3* acetylcholine receptors in xenopus laevis oocytes achieved through subunit chimeras and concatamers. *Mol. Pharmacol.* **79,** 126–140
45. Abreo, M. A., Lin, N.-H., Garvey, D. S., Gunn, D. E., Hettinger, A.-M., Wasicak, J. T., Pavlik, P. A., Martin, Y. C., Donnelly-Roberts, D. L., Anderson, D. J., Sullivan, J. P., Williams, M., Arneric, S. P., and Holladay, M. W. (1996) Novel 3-pyridyl ethers with subnanomolar affinity for central neu-

ronal nicotinic acetylcholine receptors. *J. Med. Chem.* **39,** 817–825
46. Xiao, Y., Fan, H., Musachio, J. L., Wei, Z. L., Chellappan, S. K., Kozikowski, A. P., and Kellar, K. J. (2006) Sazetidine-A, a novel ligand that desensitizes α4β2 nicotinic acetylcholine receptors without activating them. *Mol. Pharmacol.* **70,** 1454–1460
47. Zwart, R., Carbone, A. L., Moroni, M., Bermudez, I., Mogg, A. J., Folly, E. A., Broad, L. M., Williams, A. C., Zhang, D., Ding, C., Heinz, B. A., and Sher, E. (2008) Sazetidine-A is a potent and selective agonist at native and recombinant α4β2 nicotinic acetylcholine receptors. *Mol. Pharmacol.* **73,** 1838–1843
48. Colquhoun, D. (1998) Binding, gating, affinity and efficacy: the interpretation of structure-activity relationships for agonists and of the effects of mutating receptors. *Br. J. Pharmacol.* **125,** 924–947
49. Moroni, M., Vijayan, R., Carbone, A., Zwart, R., Biggin, P. C., and Bermudez, I. (2008) Non-agonist-binding subunit interfaces confer distinct functional signatures to the alternate stoichiometries of the α4β2 nicotinic receptor: an α4-α4 interface is required for Zn^{2+} potentiation. *J. Neurosci.* **28,** 6884–6894
50. Hsiao, B., Mihalak, K. B., Magleby, K. L., and Luetje, C. W. (2008) Zinc potentiates neuronal nicotinic receptors by increasing burst duration. *J. Neurophysiol.* **99,** 999–1007
51. Dash, B., Bhakta, M., Chang, Y., and Lukas, R. J. (2011) Identification of N-terminal extracellular domain determinants in nicotinic acetylcholine receptor (nAChR) α6 subunits that influence effects of wild-type or mutant β3 subunits on function of α6β2*- or α6β4*-nAChR. *J. Biol. Chem.* **286,** 37976–37989
52. Dash, B., and Lukas, R. J. (2012) Modulation of gain-of-function α6*-nicotinic acetylcholine receptor by β3 subunits. *J. Biol. Chem.* **287,** 14259–14269
53. Dash, B., Li, M. D., and Lukas, R. J. (2014) Roles for N-terminal extracellular domains of nicotinic acetylcholine receptor (nAChR) β3 subunits in enhanced functional expression of mouse α6β2β3- and α6β4β3-nAChRs. *J. Biol. Chem.* **289,** 28338–28351
54. Shahsavar, A., Ahring, P. K., Olsen, J. A., Krintel, C., Kastrup, J. S., Balle, T., and Gajhede, M. (2015) AChBP engineered to mimic the α4-β4 binding pocket in α4β2 nicotinic acetylcholine receptors reveals interface specific interactions important for binding and activity. *Mol. Pharmacol.* **88,** 697–707